Search for planetary-mass ultracompact binaries using data from the first part of the LIGO–Virgo–KAGRA fourth observing run

A. G. Abac *et al.*[*]
(The LIGO Scientific Collaboration, the Virgo Collaboration, and the KAGRA Collaboration Collaboration)

(Received 5 December 2025; accepted 8 May 2026; published 24 July 2026)

We present a search for gravitational waves from inspiraling, planetary-mass ultracompact binaries using data from the first part of the fourth observing run of LIGO, Virgo, and KAGRA. Finding no evidence of such systems, we determine the maximum distance reach for such objects and their merger rate densities. Then, we identify classes of primordial black hole mass distributions for which these rate limits can be translated into relevant constraints on the mass distribution of primordial black holes, assuming that they are all composed of dark matter, in the mass range $[10^{-6}, 10^{-3}]M_\odot$. Our constraints for the class of primordial black hole mass distribution functions $f(m)$ we consider reach down to $f(m) \sim 0.1$. They are consistent with existing microlensing results in the planetary-mass range, provide a complementary probe to subsolar mass objects, and are publicly available [1].

DOI: 10.1103/s551-7pch

I. INTRODUCTION

Black holes can form in the Universe from the core collapse of stars, or the merging of neutron stars or black holes. Since 2015, numerous gravitational wave (GW) observations have allowed us to probe these formation channels and revealed unexpected features [2–13], such as low effective spins, black holes in the low-mass gap ($[3, 5]M_\odot$) [14], in the pair-instability mass gap [15], or with very unequal mass ratios [16,17]. Though a fraction of these could come from primordial black holes (PBHs), formed through the gravitational collapse of inhomogeneities in the early Universe [18–22], uncertainties in the astrophysical and primordial formation scenarios and rates are too large to be able to disentangle the two populations.

A relatively unambiguous way to discover a PBH would be to detect a subsolar mass black hole. Matched filtering has been used to search for PBHs between $[0.1, 1]M_\odot$ in equal-mass systems and down to $0.01M_\odot$ in asymmetric mass-ratio systems, which has resulted in upper limits on the abundance of PBHs in the Universe [23–29]. Probing below $0.1M_\odot$, however, has been challenging for matched filtering because longer signal durations—$\mathcal{O}(\text{hours} - \text{days})$ versus $\mathcal{O}(100\ \text{s})$—lead to an insurmountable number of templates to analyze. These difficulties have motivated the development of time-frequency domain methods to probe PBHs with masses between $[10^{-7}, 10^{-2}]M_\odot$ [30–35], which have been used [36] to obtain the GW constraints on planetary-mass PBHs using data from the third observing run of LIGO, Virgo, and KAGRA [37–39]. Another possibility is to search for the continuous, almost monochromatic GW signal from the early inspiral of planetary-mass PBH binaries within our galaxy [40–42].

In this paper, we use data of the first part of the fourth observing run of LIGO, Virgo, and KAGRA to search for GWs from inspiraling PBH binaries. This work advances beyond previous studies not only through the use of new data, but also by identifying some relevant classes of PBH mass functions for which we obtain a significant constraint on the fraction of dark matter (DM) these PBHs could compose. Additionally, we consider the impact of binary eccentricity on our constraints.

II. THE SIGNAL

Inspiraling compact objects will lose orbital energy via GW emission, causing their orbit to shrink over time. When the objects are far from merger, we can write how quickly the GW frequency changes over time, i.e., the spin-up $\dot{f}$, as [43]

$$\dot{f}_{\rm GW} = \frac{96}{5}\pi^{8/3}\left(\frac{G\mathcal{M}}{c^3}\right)^{5/3} f_{\rm GW}^{11/3} \simeq 1.25 \times 10^{-4}\ \text{Hz/s}\left(\frac{\mathcal{M}}{10^{-3}M_\odot}\right)^{5/3}\left(\frac{f_{\rm GW}}{100\ \text{Hz}}\right)^{11/3}, \tag{1}$$

[*]Full author list given at the end of the article.

Published by the American Physical Society under the terms of the Creative Commons Attribution 4.0 International license. Further distribution of this work must maintain attribution to the author(s) and the published article's title, journal citation, and DOI.

where $\mathcal{M} \equiv \frac{(m_1 m_2)^{3/5}}{(m_1+m_2)^{1/5}}$ is the chirp mass of the system composed of objects with component masses m_1, m_2, $f_{\rm GW}$ is the GW frequency, c is the speed of light, and G is Newton's gravitational constant. We can then integrate Eq. (1) over time to obtain how the GW frequency changes with time t,

$$f_{\rm GW}(t) = f_0 \left[1 - \frac{8}{3} k f_0^{8/3} (t - t_0)\right]^{-\frac{3}{8}}, \tag{2}$$

where t_0 is a reference time for the GW frequency f_0, and $k \equiv \frac{96}{5}\pi^{8/3}(\frac{G\mathcal{M}}{c^3})^{5/3}$ is a proportionality constant. Equation (1) contains only the leading-order term in the post-Newtonian (PN) expansion. However, the impact of higher-order PN corrections on the signal's time-frequency evolution is negligible for the nonspinning, widely separated binaries considered here. We discuss how this approximation affects our upper limits in Sec. IV.

The amplitude $h_0(t)$ of the GW signal also evolves with time [43],

$$\begin{aligned} h_0(t) &= \frac{4}{d}\left(\frac{G\mathcal{M}}{c^2}\right)^{5/3}\left(\frac{\pi f_{\rm GW}(t)}{c}\right)^{2/3} \\ &\simeq 2.56 \times 10^{-23}\left(\frac{1\ \text{kpc}}{d}\right)\left(\frac{\mathcal{M}}{10^{-3} M_\odot}\right)^{5/3}\left(\frac{f_{\rm GW}(t)}{100\ \text{Hz}}\right)^{2/3}, \end{aligned} \tag{3}$$

where d is the luminosity distance to the source.

To determine how long the inspiraling systems considered in this paper will emit GWs, we can invert Eq. (2) to obtain the time to coalescence $t_{\rm coal}$ and let $f_{\rm GW}(t) \to \infty$,

$$\begin{aligned} t_{\rm coal} &\simeq \frac{5}{256}\left(\frac{1}{\pi f_0}\right)^{8/3}\left(\frac{c^3}{G\mathcal{M}}\right)^{5/3} \\ &\simeq 3.4\ \text{days}\left(\frac{100\ \text{Hz}}{f_0}\right)^{8/3}\left(\frac{10^{-3} M_\odot}{\mathcal{M}}\right)^{5/3}. \end{aligned} \tag{4}$$

We term these intermediate-duration signals lasting hours-days "transient continuous waves,"[1] whose chirp masses would range from $\mathcal{O}(10^{-5}$–$10^{-2})M_\odot$. Systems whose chirp masses are less than $10^{-5} M_\odot$ could spend years in the LIGO-Virgo-KAGRA frequency band, and are termed "continuous waves"—analogous to canonical GW emission from nonaxisymmetric rotating neutron stars [45]—and were also searched for in this dataset [46].

III. THE SEARCH

A. Data

We consider data from the first part of the fourth observing run of the LIGO Livingston (L1) and Hanford (H1) detectors, called O4a.[2] This observing run is more sensitive than previous ones across the full frequency band, but particularly at high frequencies [48–50]. Data were collected between 24 May 2023 15:00:00 UTC and 16 January 2024 16:00:00 UTC, with L1 and H1 online for 69% and 67.5% of that time, respectively. The data are calibrated [51–53] such that, at worst, amplitude and phase uncertainties at 1σ are 10% and 10 degrees, respectively. We used data from times at which the interferometers were in "science mode" [54]. Virgo did not operate during O4a, while KAGRA observed for one month.

The data structures that we used as the input to this search are called short fast Fourier transform databases [55,56], which contain frequency-domain representations of the data every ∼17 minutes that are cleaned of short time-domain disturbances ("glitches") [55]. Because we require the fast Fourier transform (FFT) length $T_{\rm FFT} \ll 17$ minutes, we inverse Fourier transform the data to the time domain and create new time-frequency representations of the data with the desired $T_{\rm FFT}$.

B. Method

Standard searches for compact binary coalescences use matched filtering to coherently match signal waveforms to GW data. Such analyses work well for short-duration signals, but for the long-duration signals present here, matched filtering would be computationally infeasible, thus, we employ a *semicoherent* approach. We break the data into coherent chunks of length $T_{\rm FFT}$, and sum the power across different FFTs incoherently. Such *semicoherent* searches require a choice of $T_{\rm FFT}$ that ensures that the GW frequency is monochromatic during each FFT. Practically, $T_{\rm FFT}$ is a function of $\mathcal{M}$, $f_{\rm GW}$, and the signal duration $T_{\rm PM}$, as described in Sec. III C.

Here, we use the *generalized frequency–Hough* to search for GWs from inspiraling compact objects [30,34,57–60]. For a given power-law model of the time-frequency evolution of the signal [Eq. (2)], the *generalized frequency–Hough* operates on a time-frequency representation of the data called the *peakmap* (PM), a collection of ones and zeros that indicates the particular frequencies whose power is a local maximum and greater than a chosen threshold. This method performs a transformation from the $t - f_{\rm GW}$ plane of each detector separately to the $f_0 - \mathcal{M}$ plane of the source. In doing this transformation, we sum over different possible tracks in the time-frequency plane to accumulate the "peaks" (the ones) corresponding to specific chirp masses and coalescence times. The number of unique tracks to search over depends on our analysis parameters—$T_{\rm FFT}$, $T_{\rm PM}$—and $f_{\rm GW}$.

In contrast to previous searches, we use *generalized frequency–Hough*-v2 that is approximately an order of

[1]This term was coined originally in the context of signals arising after pulsar glitches [44].

[2]We used the channel GDS–CALIB_STRAIN_CLEAN_AR with CAT1 vetoes [47].

magnitude faster than previous versions [58–60], permitting us to perform an extensive follow-up campaign of significant time-frequency tracks.

C. Parameter space construction

We perform the search in a number of "configurations," where each configuration corresponds to a particular frequency band $[f_{\min}, f_{\max}]$, T_{FFT}, a *peakmap* duration T_{PM}, and a chirp mass range $[\mathcal{M}_{\min}, \mathcal{M}_{\max}]$. These parameters are chosen to maximize the sensitivity, i.e., the distance reach Eq. (B1), toward systems with chirp masses between $[\mathcal{M}_{\min}, \mathcal{M}_{\max}]$ by considering the changing noise power spectral density of the interferometers, the varying amplitude of the signal over time, and the steep increase in $\dot{f}$ over time, which results in a decrease of the analysis coherence time if we wish to confine the signal power to one frequency bin during T_{FFT}. By looping over all possible chirp masses and GW frequencies, we can empirically determine these parameters by calculating the distance reach, and grouping nearby points in the parameter space to be searched for in a single *peakmap* with the criterion that no more than 10% sensitivity is lost with respect to creating separate *peakmaps* for each of those nearby points. To limit the computational cost of the search, we require that the chosen parameters would lead to detectable signals at least 0.1 kpc from us, and the Doppler shift induced by the relative motion of the Earth and source is confined to one frequency bin for the signal duration.

At the end of this process, we obtain 685 unique configurations with $T_{\mathrm{FFT}} \in [2, 13]$ s and $T_{\mathrm{PM}} \in [2.3\mathrm{h}, 6.75\mathrm{d}]$ covering systems with $\mathcal{M} \in [10^{-5}, 10^{-2}] M_{\odot}$.

D. Results

We perform the *generalized frequency–Hough* on each *peakmap* in each configuration per detector separately, across the whole observing run $T_{\mathrm{obs}} \simeq 8$ months. Candidates returned from each detector with similar chirp masses and coalescence times are considered "significant" and "in coincidence" if (1) their parameters do not differ by more than three bins in the two-dimensional $f_0 - \mathcal{M}$ parameter space, (2) their detection statistics, called the "critical ratio" (*CR*), are comparable (within 20% of each other), (3) their average *CR* exceeds a threshold of ∼7 determined by the trials factor and assuming Gaussian noise, and (4) their time-frequency tracks do not overlap by more than 30% with a known noise line [47,61]. The *CR* threshold is set taking into account computing power constraints: the follow-up can be an expensive portion of the search, because the demodulation procedure, discussed below, is very sensitive to parameter uncertainties and T_{FFT} [57,62].

The chosen criteria lead to a manageable 5×10^5 candidates. These candidates were subject to a follow-up procedure in which the original time-series data were demodulated based on the expected phase evolution of the signal, obtained by integrating Eq. (2). Such a demodulation will ideally ensure the signal remains monochromatic during its duration, thus permitting us to use a longer coherence time.

We then compute a new time-frequency *peakmap* after doubling T_{FFT}, and apply the *frequency-Hough* [62–64], which searches over residual $\dot{f}_{\mathrm{GW}}$ that may occur for imperfect corrections. Similarly to the *generalized frequency–Hough*, the *frequency-Hough* maps points in the t-f_{GW} plane of the detector to lines in the f_0-$\dot{f}_{\mathrm{GW}}$ plane of the source. We only require that the new *CR* exceeds the previously found *CR* by any amount, which would occur for a real GW signal because the coherence time has been increased.

The parameters returned by the *frequency-Hough* are then used to correct the *peakmap* for any residual modulations, which would lead to a monochromatic signal, then, the *peakmap* is projected onto the frequency axis. At this stage, a new *CR* is calculated on the projected *peakmap*, and that *CR* must exceed the previously calculated *CR* in order for a candidate to be subject to further analysis. Nineteen candidates survived one doubling of T_{FFT} until the *peakmap* projection, after which all were vetoed. See Appendix A for more details regarding the final stages of the search and the threshold selection, and previous methods papers for graphical descriptions of the follow-up methods, e.g., [34,57,65].

IV. UPPER LIMITS

A. Computing expected distance reach

The procedure for semianalytically computing upper limits on the search's distance reach is described elsewhere [34] and was used in [36], so we highlight only the important aspects here and provide more details in Appendix B. Although all coincident candidates have been vetoed, we can still use their *CR* values as thresholds to estimate the distance from which a real signal could have originated in order to not produce a *CR* larger than that observed in H1 and L1. If a GW arising from a source a certain distance away can pass these thresholds at least 95% of the time, we can set an upper limit on the distance reach for sources similar to that particular candidate $d_{\mathrm{max,95\%}}$ at which 95% of injections would be detected, i.e., at a particular time, frequency range, and chirp mass. We can compute $d_{\mathrm{max,95\%}}$ in two ways: (1) by requiring that an injected GW signal in the data be recovered with a *CR* larger than that returned in both H1 and L1 95% of the time, or (2) by analytically calculating the distance reach as a function of the coincident candidates returned in the search. We choose to do the latter, but verify that both approaches produce consistent $d_{\mathrm{max,95\%}}$ upper limits—see Appendix B.

For each of the coincident candidates in each configuration before thresholding the detection statistic, we compute $d_{\mathrm{max,95\%}}$. To be conservative, we use the maximum

detection statistic of coincident candidates returned in H1 and L1, and apply the Feldman-Cousins procedure to it [66], effectively increasing the *CR*, thus reducing the distance reach.

In each configuration, we compute the mean and standard deviation of the distance reaches over different detector times and frequencies, which accounts for the varying power spectral density. Among all configurations, we take the maximum distance reach at each chirp mass. We also require that the time-frequency track of each candidate within T_{PM} differs by no more than one frequency bin from the time-frequency track that the signal would follow at 3.5PN,

$$|f_{\mathrm{GW}}(t) - f_{3.5\mathrm{PN}}(t)| \leq \frac{1}{T_{\mathrm{FFT}}}, \tag{5}$$

where $f_{3.5\mathrm{PN}}(t)$ is given by Eq. (5.258) in [43]. This criterion has a bigger impact on the allowed candidates to contribute to the upper limits for asymmetric mass-ratio systems, since the mass ratio enters at 1PN.

Our search is sensitive to ultracompact objects inspiraling for which $\mathcal{M} \in [10^{-5}, 10^{-2}]M_{\odot}$, and whose time-frequency evolution follow Eq. (2). Thus, we provide in Fig. 1 constraints on the distance reach $d_{\mathrm{max,95\%}}$ for equal-mass systems that are independent of the nature of the compact objects and of the binary formation model. From Eq. (B1), a power-law behavior of $d_{\mathrm{max,95\%}} \propto \mathcal{M}^{5/4}$ is expected. Fitting the curve, we find a power-law index of 1.24, within 1% from the theoretical value.

The procedure used to calculate $d_{\mathrm{max,95\%}}$ has been validated through injection studies in both O3 [34] and O4a (see Appendix B), in which we have tested performance across different times and frequency bands at fixed chirp mass. Its robustness to variations in curvature within the time-frequency plane is further supported by previous injection campaigns targeting rapidly spinning down-isolated neutron stars in O2 [57,67]. In those studies, the algorithm tracked signals following distinct power-law time-frequency evolutions with sensitivities consistent with Eq. (B1). Together, these results demonstrate that the *generalized frequency–Hough* performs reliably across a broad range of chirping signals.

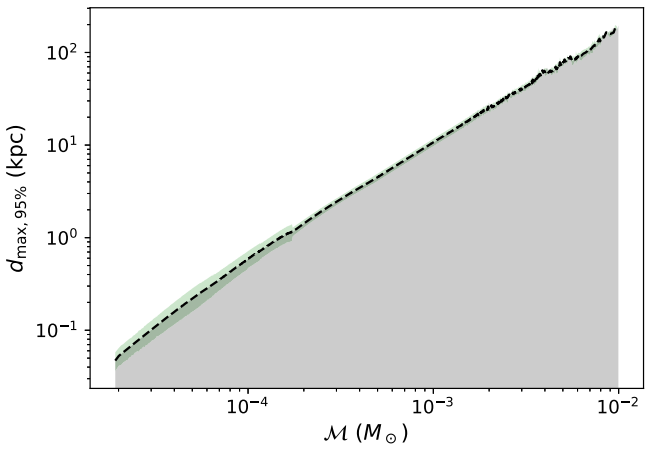

FIG. 1. Model-independent distance reach constraints for equal-mass inspiraling compact objects. We show the distance reach at which 95% of signals would be recovered for equal-mass systems. The green shaded region denotes 1 standard deviation uncertainty on the distance reach, while the gray-shaded region indicates excluded distances. These constraints follow the expected power law of $d_{\mathrm{max,95\%}} \propto \mathcal{M}^{5/4}$.

B. Computing upper limits on merger rate density

We set upper limits on the merger rate density in a different way than what is done to obtain $d_{\mathrm{max,95\%}}$. This is because $d_{\mathrm{max,95\%}}$ is calculated based on the returned coincident candidates in the search. We set upper limits on rate density not via $d_{\mathrm{max,95\%}}$ to account for the differences between our analysis and those in matched-filter subsolar mass searches [23–29].

We note that, in standard subsolar mass searches [23–29], the loudest event across the whole parameter space is used to set upper limits on rate density, which follows the formalism in [68–70]. These are *globally* conservative upper limits.

However, our search differs because the detection statistic (the *CR*) is updated throughout the follow-up procedure. Additionally, the coincident candidates have all been shown to be due to noise disturbances in the follow-up (see Appendix A and the figures therein for details on these *CR*s.) In essence, the threshold that we set on our statistic, $CR_{\mathrm{thr}} = 7$, sets the sensitivity floor of the search: signals with $CR > CR_{\mathrm{thr}}$ enter the follow-up stage and can be detected, while signals with $CR < CR_{\mathrm{thr}}$ are lost. Thus, we can compute the upper limits on rate density by noting that the probability density function of a certain value of the *CR*, given that it originates from a signal at a distance r away, is

$$p(CR|r) = \frac{1}{\sqrt{2\pi}} e^{-(CR-(D/r)^2)^2/2}, \tag{6}$$

where D is the collection of prefactors that denote the distance away we could detect a signal as a function of the chirp mass, the frequencies covered by the signal, and our analysis parameters T_{FFT}, T_{obs},

$$D = 1.41 \left(\frac{G\mathcal{M}}{c^2}\right)^{5/3} \left(\frac{\pi}{c}\right)^{2/3} \frac{T_{\mathrm{FFT}}}{{T_{\mathrm{PM}}}^{1/2}} \times \left(\sum_x^N \frac{f_{\mathrm{GW},x}^{4/3}}{S_n(f_{\mathrm{GW},x})}\right)^{1/2} \left(\frac{p_0(1-p_0)}{N p_1^2}\right)^{-1/4}. \tag{7}$$

See Appendix B for the full equation and its validation against injections. S_n is the noise power spectral density of

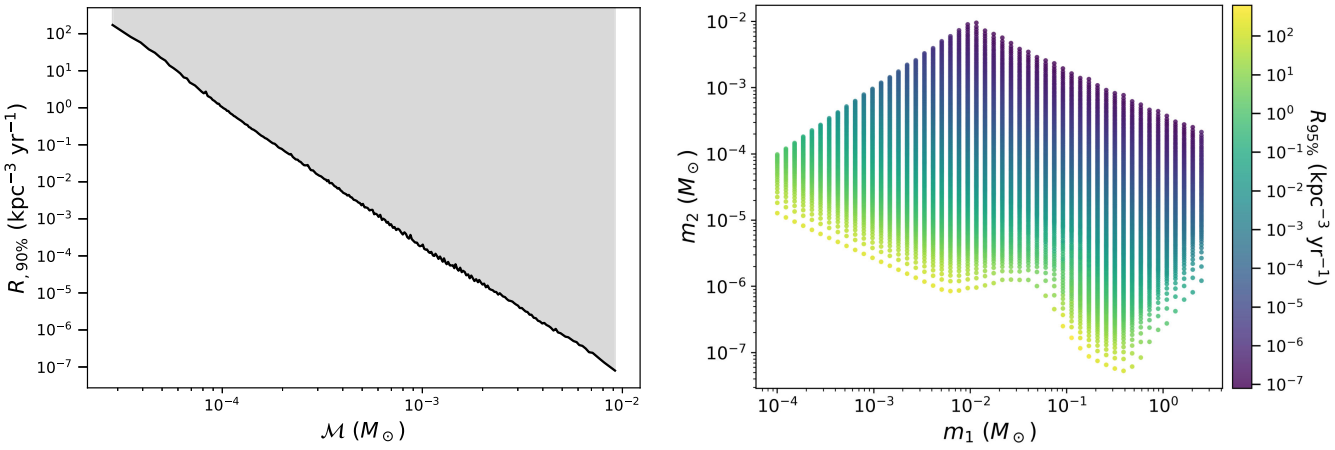

FIG. 2. Model-independent constraints on rate density at the 90% confidence level for equal-mass (left) and asymmetric mass-ratio inspiraling compact objects (right). These constraints are derived following the procedure outlined in Sec. IV B, and obey the expected power law of $\mathcal{R} \propto \mathcal{M}^{-15/4}$.

the H1 or L1, $N = T_{\rm obs}/T_{\rm FFT}$, and p_0 and p_1 are given in Eq. (B2) and (B3). The integral of Eq. (6) gives the efficiency $\epsilon(r)$,

$$\epsilon(r) = P(CR > CR_{\rm thr}|r) = \frac{1}{2}\mathrm{erfc}\left(\frac{CR_{\rm thr} - \left(\frac{D}{r}\right)^2}{\sqrt{2}}\right). \tag{8}$$

Then, the comoving spacetime volume $\langle VT\rangle$ can be approximated using Laplace's method (see Appendix C for more details),

$$\begin{aligned}\langle VT\rangle &= T_{\rm obs}\int_0^\infty 4\pi r^2 \epsilon(r) dr \\ &\simeq T_{\rm obs}\frac{4}{3}\pi\left(\frac{D}{\sqrt{CR_{\rm thr}}}\right)^3.\end{aligned} \tag{9}$$

Assuming that the event rate for inspiraling ultracompact objects is Poissonian, consistent with other searches [24,25,28], we can then calculate the upper limits on the rate density at a chosen confidence level $\alpha = 0.9$,

$$\mathcal{R}_{90\%} = \frac{2.303}{\langle VT\rangle}. \tag{10}$$

We show our upper limits on $\mathcal{R}_{90\%}$ in Fig. 2 for equal-mass and asymmetric mass-ratio systems. The rate density follows a power law of approximately $\mathcal{R} \propto D^{-3} \propto \mathcal{M}^{-15/4}$. From fitting the curve, we find the power-law index to be–3.66, a 2% difference.

C. Model-dependent constraints on PBHs

Translating these constraints into limits on the PBH abundance is subtle and highly model dependent. Indeed, several binary formation channels have been proposed and each of them depend on the PBH mass distribution and are subject to multiple astrophysical uncertainties. Following state-of-the-art rate prescriptions [71], early-Universe two-body binaries are typically the dominant binary formation channel for the masses and DM fraction relevant for this work. Their merger rate densities $\mathcal{R}^{\rm cos}_{\rm prim}$ are given by

$$\begin{aligned}\mathcal{R}^{\rm cos}_{\rm prim} &\approx 1.6\times 10^{-12}\ \mathrm{kpc^{-3}\,yr^{-1}}\,\tilde{f}^{53/37} \\ &\times\left(\frac{m_1+m_2}{M_\odot}\right)^{-32/37}\left[\frac{m_1 m_2}{(m_1+m_2)^2}\right]^{-34/37},\end{aligned} \tag{11}$$

where we define an effective parameter $\tilde{f}$ as

$$\tilde{f} \equiv f_{\rm PBH}[f_{\rm sup} f(\ln m_1)\Delta\ln m_1 f(\ln m_2)\Delta\ln m_2]^{37/53}, \tag{12}$$

where $f(\ln m)$ is the PBH mass probability density function, normalized such that $\int f(\ln m) d\ln m = 1$. $f_{\rm PBH}$ is the total fraction of DM made of PBHs and $f_{\rm sup}$ is a merger rate suppression factor (= 1 if no suppression) that accounts for the various mechanisms affecting the binary orbital properties throughout the history of the Universe [72], changing their merger time or destroying them.[3] Constraining $\tilde{f}$ eliminates the dominant sources of uncertainty, namely those arising from the suppression factor and the mass distribution. In the following, we will identify conditions on the mass distributions for which the suppression is minimal, which is required to lead to relevant constraints.

[3]The fraction of PBHs that originally form in binaries versus as isolated systems is accounted for in the derivation of Eq. (11).

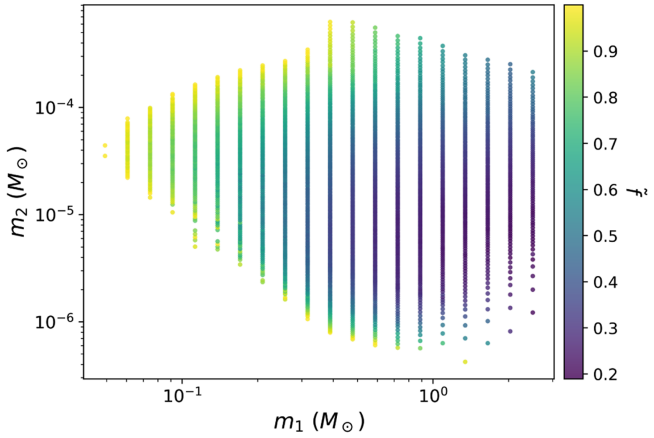

FIG. 3. Model-dependent constraints on asymmetric mass-ratio inspiraling PBHs. We interpret the rate densities in Fig. 2(b) as arising from PBHs, and constrain the effective parameter $\tilde{f}$ as a function of asymmetric mass-ratio PBHs using Eq. (14). We restrict the plot only to masses for which $\tilde{f} < 1$, and note that we were unable to constrain $\tilde{f} < 1$ for equal-mass systems.

Compared to standard compact binary coalescence searches, the distance is limited to our galactic environment. One therefore has to translate cosmological merger rates into galactic rates, taking into account the galactic DM density profile. If the galactic DM density was the one at the Sun's location, $\rho_{\rm DM} \simeq 10^{16} M_\odot {\rm Mpc}^{-3}$ [73], the merger rates would be enhanced to $\mathcal{R} = 3.3 \times 10^5 \mathcal{R}^{\rm cos}_{\rm prim}$ [30]. However, with O4a data, we can probe source distances comparable to the distance to the Galactic Center from Earth. We therefore have modified the rates by a factor $F(d)$ that accounts for the integrated DM density profile centered on the Sun's location at 8.2 kpc from the Galactic Center, as described in the Appendix D. Thus, we rewrite Eq. (11) in both the equal-mass case

$$\mathcal{R} = 1.04 \times 10^{-6}\ {\rm kpc}^{-3}\,{\rm yr}^{-1} F(d) \left(\frac{M_{\rm PBH}}{M_\odot}\right)^{-32/37} \tilde{f}^{53/37}, \tag{13}$$

where $M_{\rm PBH} = 2^{1/5}\mathcal{M}$, and the asymmetric mass-ratio case

$$\mathcal{R} = 5.28 \times 10^{-7}\ {\rm kpc}^{-3}\,{\rm yr}^{-1} \times F(d) \left(\frac{m_1}{M_\odot}\right)^{-32/37} \left(\frac{m_2}{m_1}\right)^{-34/37} \tilde{f}^{53/37}, \tag{14}$$

defining $m_2 < m_1$.

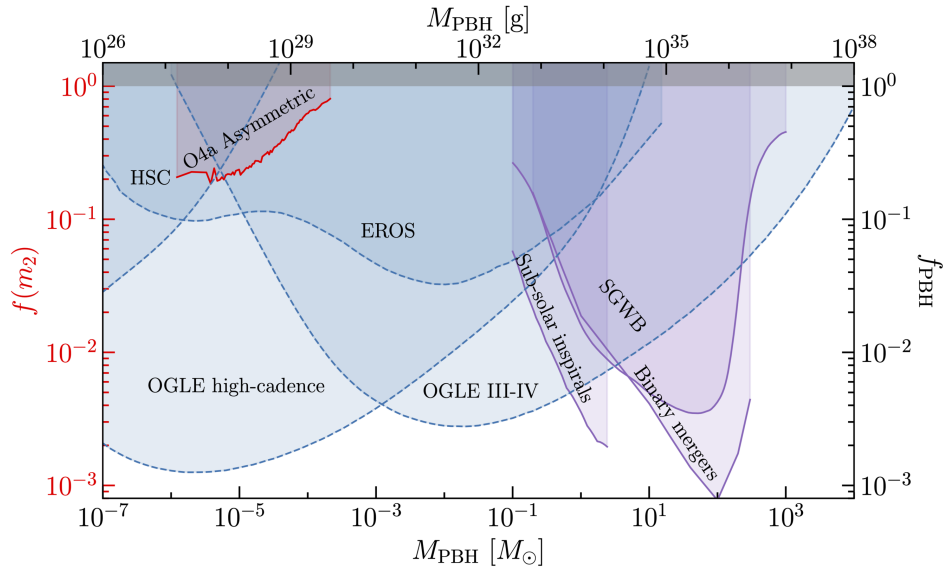

FIG. 4. Constraints on PBHs from this search, in red, and other GW and electromagnetic analyses. Our limits on the mass function $f(m_2)$ [shorthand for $f(\ln m_2)$] are valid for mass distributions respecting the conditions mentioned in the text for asymmetric mass ratio binaries, assuming $f_{\rm PBH} = 1$. No curve is shown for equal-mass systems, as $\tilde{f} < 1$ is not constrained. We assume $f(\ln m_1)\Delta \ln m_1 \sim 1$ and use the corresponding values of $\tilde{f}$ in Fig. 3 at $m_1 = 2.5 M_\odot$ to obtain the red line on this plot. We emphasize that these constraints are valid only for the classes of mass functions discussed in Sec. IV D. If one wishes to produce our constraints for different choices of $f_{\rm PBH}$, the red curve will be scaled upwards by $f_{\rm PBH}^{-53/37}$. Constraints from other probes (microlensing and GWs) are also presented for comparison on $f_{\rm PBH}$, and are implicitly valid for monochromatic mass functions and subject to astrophysical uncertainties. Purple curves correspond to constraints from previous GW searches [23,24,29,75–79], while dashed blue curves indicate microlensing constraints [80–83] that could weaken significantly due to PBH clustering depending on the assumed PBH formation model, mass of the cluster, and the distributions of DM density and velocity [84,85]. Our constraints on the mass function in red should be referenced to the red left y-axis, while all other constraints are directly on $f_{\rm PBH}$ and should be referenced to the right y-axis.

In Fig. 3, we show the constraints on $\tilde{f}$ in the asymmetric mass-ratio case inferred from Fig. 2(b) (we do not find relevant constraints in the equal-mass case).

D. Constraining $f_{\rm PBH}$ from $\tilde{f}$

Though we constrain the effective parameter $\tilde{f}$ down to about 0.2 in a portion of the parameter space for asymmetric mass-ratio binaries, in order to derive a meaningful limit on $f_{\rm PBH}$, given Eq. (11), we need to find regimes in which $f_{\rm sup} \gtrsim 0.04$ or even close to unity. We identify below some general conditions on the mass distribution for which this is satisfied for asymmetric mass-ratio binaries, and provide further details in the Appendix D for equal-mass systems, which remain unconstrained in this analysis. We choose our mass distributions to avoid cases of binary formation suppression [$f_{\rm sup} \sim \mathcal{O}(1)$], however, to constrain alternative mass functions, the methodology outlined in this subsection can be followed.

For asymmetric mass-ratio binaries, we can constrain $f_{\rm PBH}^{53/37} f(\ln m_2)$, under some sufficient conditions: (i) if there is a peak in the distribution at the mass m_1, such that $f(\ln m_1)\Delta \ln m_1 \approx 1$ and the mean PBH mass is $\langle m \rangle \approx m_1$, and (ii) if there is at least a small DM fraction in heavy black holes, enough to seed PBH clusters, such that the binary is unlikely to be perturbed by other PBHs. In this case, we obtain $f_{\rm sup} \approx 0.5$ and can constrain $f(\ln m_2)$ in the range $10^{-6} < m_2/M_\odot < 10^{-4}$, if m_1 is at the solar-mass scale, as expected in the motivated class of mass functions imprinted by the QCD epoch [74]. The most stringent limit on $f(\ln m_2)$ is when one assumes $f_{\rm PBH} = 1$, but one should note that this would be in conflict with existing limits. We show these limits on $f(\ln m_2)$ assuming $f_{\rm PBH} = 1$ in Fig. 4, which can be compared to existing experiments.

V. CONCLUSIONS

We have performed a search for planetary-mass, ultracompact objects using data from the first part of the LIGO, Virgo, and KAGRA fourth observing run. Though we did not find any significant events, we placed upper limits on both the distance reach and merger rate density of equal-mass and asymmetric mass-ratio ultracompact binaries. Moreover, for certain classes of formation models, we constrain the fraction of DM that PBHs could compose for asymmetric mass-ratio systems. Our work complements matched filtering searches for subsolar mass PBH binaries by considering lower-mass regimes that would require too much computational power to analyze with matched filtering. Our results provide a complementary way to probe planetary-mass PBH binaries that could form in clusters. In Fig. 4, we show how our bounds on $f(\ln m_2)$ compare to other observations, assuming $f_{\rm PBH} = 1$. We also find that our constraints are valid for systems with eccentricities as high as 0.84 (see Appendix E for more details). Note that each method has its own systematics and assumptions, and it may happen that microlensing constraints weaken due to a better understanding of the galactic rotation curves [86], which strengthens the argument that we need multiple probes of PBHs in this mass regime. Moreover, we note that PBH physics is an evolving field: while we consider particular mass functions and conditions to arrive at Fig. 4, we emphasize that these limits could change with time, and that different assumptions could lead to different constraints. Hence, we release the rate density constraints directly to allow readers to choose their own ways of interpreting our results, along with codes to generate these plots [1,87–89].

As we look forward to future ground- and space-based GW interferometers that will probe even lower frequencies than accessible now, the impact of eccentricity on the inspiral signal will become even more significant. Waveforms to handle eccentricity [90–99] and DM effects [100–106] in matched filtering analyses are currently under development, but these effects will not impact semicoherent analyses, such as the *generalized frequency–Hough*, as much. Our analysis thus allows us to be sensitive to a range of rich physics while maintaining computational efficacy.

ACKNOWLEDGMENTS

This material is based upon work supported by NSF's LIGO Laboratory, which is a major facility fully funded by the National Science Foundation. The authors also gratefully acknowledge the support of the Science and Technology Facilities Council (STFC) of the United Kingdom, the Max-Planck Society (MPS), and the State of Niedersachsen/Germany for support of the construction of Advanced LIGO and construction and operation of the GEO 600 detector. Additional support for Advanced LIGO was provided by the Australian Research Council. The authors gratefully acknowledge the Italian Istituto Nazionale di Fisica Nucleare (INFN), the French Centre National de la Recherche Scientifique (CNRS), and the Netherlands Organization for Scientific Research (NWO) for the construction and operation of the Virgo detector and the creation and support of the EGO consortium. The authors also gratefully acknowledge research support from these agencies as well as by the Council of Scientific and Industrial Research of India, the Department of Science and Technology, India, the Science and Engineering Research Board (SERB), India, the Ministry of Human Resource Development, India, the Spanish Agencia Estatal de Investigación (AEI), the Spanish Ministerio de Ciencia, Innovación y Universidades, the European Union NextGenerationEU/PRTR (PRTR-C17.I1), the ICSC–CentroNazionale di Ricerca in High Performance Computing, Big Data and Quantum Computing, funded by the European Union NextGenerationEU, the Comunitat Autonòma de les Illes Balears through the Conselleria d'Educació i Universitats, the Conselleria d'Innovació, Universitats, Ciència i Societat Digital de la Generalitat

Valenciana and the CERCA Programme Generalitat de Catalunya, Spain, the Polish National Agency for Academic Exchange, the National Science Centre of Poland and the European Union—European Regional Development Fund; the Foundation for Polish Science (FNP), the Polish Ministry of Science and Higher Education, the Swiss National Science Foundation (SNSF), the Russian Science Foundation, the European Commission, the European Social Funds (ESF), the European Regional Development Funds (ERDF), the Royal Society, the Scottish Funding Council, the Scottish Universities Physics Alliance, the Hungarian Scientific Research Fund (OTKA), the French Lyon Institute of Origins (LIO), the Belgian Fonds de la Recherche Scientifique (FRS-FNRS), Actions de Recherche Concertées (ARC) and Fonds Wetenschappelijk Onderzoek—Vlaanderen (FWO), Belgium, the Paris Île-de-France Region, the National Research, Development and Innovation Office of Hungary (NKFIH), the National Research Foundation of Korea, the Natural Sciences and Engineering Research Council of Canada (NSERC), the Canadian Foundation for Innovation (CFI), the Brazilian Ministry of Science, Technology, and Innovations, the International Center for Theoretical Physics South American Institute for Fundamental Research (ICTP-SAIFR), the Research Grants Council of Hong Kong, the National Natural Science Foundation of China (NSFC), the Israel Science Foundation (ISF), the US-Israel Binational Science Fund (BSF), the Leverhulme Trust, the Research Corporation, the National Science and Technology Council (NSTC), Taiwan, the United States Department of Energy, and the Kavli Foundation. The authors gratefully acknowledge the support of the NSF, STFC, INFN, and CNRS for provision of computational resources. This work was supported by MEXT, the JSPS Leading-edge Research Infrastructure Program, JSPS Grant-in-Aid for Specially Promoted Research 26000005, JSPS Grant-in-Aid for Scientific Research on Innovative Areas 2402: 24103006, 24103005, and 2905: JP17H06358, JP17H06361, and JP17H06364, JSPS Core-to-Core Program A, Advanced Research Networks, JSPS Grants-in-Aid for Scientific Research (S) 17H06133 and 20H05639, JSPS Grant-in-Aid for Transformative Research Areas (A) 20A203: JP20H05854, the joint research program of the Institute for Cosmic Ray Research, University of Tokyo, the National Research Foundation (NRF), the Computing Infrastructure Project of the Global Science experimental Data hub Center (GSDC) at KISTI, the Korea Astronomy and Space Science Institute (KASI), the Ministry of Science and ICT (MSIT) in Korea, Academia Sinica (AS), the AS Grid Center (ASGC), and the National Science and Technology Council (NSTC) in Taiwan under grants including the Science Vanguard Research Program, the Advanced Technology Center (ATC) of NAOJ, and the Mechanical Engineering Center of KEK. Additional acknowledgements for support of individual authors may be found in the following document: [107]. For the purpose of open access, the authors have applied a Creative Commons Attribution (CC BY) license to any Author Accepted Manuscript version arising. We request that citations to this article use "A. G. Abac *et al.* (LIGO-Virgo-KAGRA Collaboration),..." or similar phrasing, depending on journal convention.

DATA AVAILABILITY

The data that support the findings of this article are openly available [59,60].

APPENDIX A: DETAILS ON FINAL STEPS OF THE SEARCH

We select the top 1% of candidates in every Hough map that is created. Each candidate is defined to have the following parameters: (1) the signal frequency at a reference time, (2) the chirp mass, and (3) the detection statistic. The analysis of each detector's data is performed separately, meaning that we can look for *coincident candidates*, i.e., candidates with similar enough parameters present at the same times in both detectors. We define "close enough" to be three bins away,

$$\mathrm{dist} = \sqrt{\left(\frac{k_{\mathrm{LHO}} - k_{\mathrm{LLO}}}{\delta k}\right)^2 + \left(\frac{z_{0,\mathrm{LHO}} - z_{0,\mathrm{LLO}}}{\delta z_0}\right)^2}, \tag{A1}$$

where δk and δz_0 are the bin sizes in each of the coordinates in the Hough map. Note that we create the Hough maps in the transformed coordinates $z = 1/f^{8/3}$ and k, not f_0 and $\mathcal{M}$—see [57] for details on this transformation. δk varies as a function of T_{FFT}, k ($\mathcal{M}$), and f_0, while δz_0 depends solely on f_0 and T_{FFT} [57].

At this stage, we apply a threshold on the critical ratio, $CR_{\mathrm{thr}} \gtrsim 7$, that ensures that we only consider candidates with a false alarm probability of 1% (accounting for the trials factor) in Gaussian noise. The data are not Gaussian, which means that we tend to keep large noise disturbances as well as potential signals. If we were to have estimated a background for the CR using time-slides or another method traditionally used in compact binary searches, we would have obtained a higher threshold than $CR_{\mathrm{thr}} \sim 7$ due to the presence of non-Gaussian noise disturbances. Thus, our threshold is conservative. We show the distribution of candidate above this threshold in Fig. 5.

The number of coincident candidates that surpass these tests is $\sim 5 \times 10^5$. Each of these candidates is subject to a follow-up procedure: the data are demodulated based on the candidate parameters, which would lead to a perfectly monochromatic signal if the demodulation was done correctly. The search is then rerun, with a new T_{FFT} equal to twice the original one. All candidates are vetoed in this

procedure, since they do not produce *CR*s that exceed those from the first stage of the search, as would be expected for a monochromatic signal with increased $T_{\rm FFT}$ length.

APPENDIX B: OBTAINING DISTANCE REACH UPPER LIMITS

We describe how we set upper limits on the model-independent distance reached as a function of chirp mass. To do so, we employ a semianalytic/data-driven procedure outlined in [34], which uses as input results from our search (detection statistics and detector power spectral density), and an equation for a theoretical sensitivity estimate of our method, as a way to obtain upper limits on the maximum distance away that we could have seen a source as a function of chirp mass, i.e., Fig. 1. Such a procedure was designed to avoid extensive injection campaigns to set upper limits and instead use that computing power to follow-up interesting candidates.

Even though each configuration is labeled by a particular chirp mass and starting frequency $(\mathcal{M}'_i, f'_{0,i})$, the *peakmaps* and Hough maps generated can actually probe many different chirp masses and starting frequencies. Let us label the space of chirp masses as $\mathcal{M}_k$. Within a given Hough map (say j) for a particular configuration (say i), all instances of $\mathcal{M}_k$ (with any starting frequency f_l) are assigned a critical ratio ($CR^{\rm IFO}_{i,j,k,l}$) per interferometer, IFO. We then compute the distance reach using Eq. (B1) for each detector separately with the following:

$$d^{\Gamma}_{\rm max} = 1.41\left(\frac{G\mathcal{M}}{c^2}\right)^{5/3}\left(\frac{\pi}{c}\right)^{2/3}\frac{T_{\rm FFT}}{{T_{\rm PM}}^{1/2}}\left(\frac{p_0(1-p_0)}{Np_1^2}\right)^{-1/4} \times\left(\sum_x^N \frac{f^{4/3}_{{\rm GW},x}}{S_n(f_{{\rm GW},x})}\right)^{1/2}(CR-\sqrt{2}{\rm erfc}^{-1}(2\Gamma))^{-1/2}, \tag{B1}$$

where $\Gamma = 0.95$ is the fraction of detectable signals in repeated experiments, $N = T_{\rm obs}/T_{\rm FFT}$ is the number of FFTs used to make the *peakmap*, and p_0 is the probability of selecting a peak above $\theta_{\rm thr} = 2.5$, the threshold on equalized power in the *peakmap*, and

$$p_0 = e^{-\theta_{\rm thr}} - e^{-2\theta_{\rm thr}} + \frac{1}{3}e^{-3\theta_{\rm thr}} \tag{B2}$$

and

$$p_1 = \theta_{\rm thr}\left(\frac{1}{2}e^{-\theta_{\rm thr}} - \frac{1}{2}e^{-2\theta_{\rm thr}} + \frac{1}{6}e^{-3\theta_{\rm thr}}\right) + \frac{1}{4}e^{-2\theta_{\rm thr}} - \frac{1}{9}e^{-3\theta_{\rm thr}} \tag{B3}$$

both relate to the probability of selecting a peak above the threshold $\theta_{\rm thr}$ in the presence of a weak monochromatic signal [108]. We note that this equation is strictly valid for signals lasting at least one sidereal day. However, since it is evaluated millions of times for coincident candidates occurring at random times in the run, the ensemble of evaluations effectively samples all sidereal phases.

In Eq. (B1), we must input a value for the *CR* that accounts for the fact that this equation was derived in the case of Gaussian noise, but our analysis was done in real noise. We first take the maximum of the two *CR*s returned from each interferometer: $CR_{i,j,k,l} = \max_{\rm IFO}(CR^{\rm IFO}_{i,j,k,l})$. This is a conservative choice, since it reduces $d^{\Gamma}_{\rm max}$ with respect to using the average or minimum *CR*.

Then, we employ the Feldman-Cousins (FC) [66] approach, in which we assume that the *CR* follows a Gaussian distribution, and map the measured $CR_{i,j,k,l}$ to a positive-definite value using the upper value of Table 10 in [66] at 95% confidence. Here, we input $CR_{i,j,k,l}$ into the Feldman-Cousins procedure. In other words, $CR_{{\rm FC},i,j,k,l} = FC(CR_{i,j,k,l})$ in Eq. (B1), which serves to reduce the distance reach with respect to if we had used just the maximum *CR* of the coincident candidates. Thus, the meaning of the upper limit is as follows: a real signal would need to have a critical ratio larger than that used in Eq. (B1) in order to be detectable in 95% of repeatable experiments, at a particular reference time, chirp mass, and frequency.

Let us call the result of inputting $CR_{{\rm FC},i,j,k,l}$ into Eq. (B1) $d^{\Gamma}_{i,j,k,l}$. For each combination of i, j, k, l—which corresponds to each coincident candidate we have in the search, before applying any threshold or follow-ups—we compute a distance reach at which 95% of signals in a repeated number of experiments would be recovered, $d^{95\%}_{i,j,k,l}$, which represents, in repeated experiments, the distance at which 95% of signals with a given chirp mass at a given time during the run would have been detected.

We then take the median of all the distances over the duration of the observing run, i.e., $d^{95\%}_{i,k} = {\rm median}(d^{95\%}_{i,j,k})$ over each set of $T_{\rm obs}/T_{\rm PM}$ values, leading to one distance reach per configuration per probed chirp mass. These denote the different sensitivities of each configuration to that particular chirp mass, some of which will be more sensitive than others. Therefore, we take the maximum of these distances for each chirp mass as the distance upper limit, i.e., $d_{{\rm max},95\%,{\rm k}} = \max(d^{95\%}_{i,k})$, which are shown in Fig. 1.

The upper limits in Fig. 1 are independent of any population or formation model for planetary-mass ultracompact objects. They indicate that a system with a given chirp mass could have been detected in 95% of repeatable experiments at a particular distance away from us.

As shown in [30,34,41,57], the use of Eq. (B1) produces consistent upper limits compared to those that would be obtained by injecting simulated signals. We also provide an injection study done in this dataset for a range of chirp

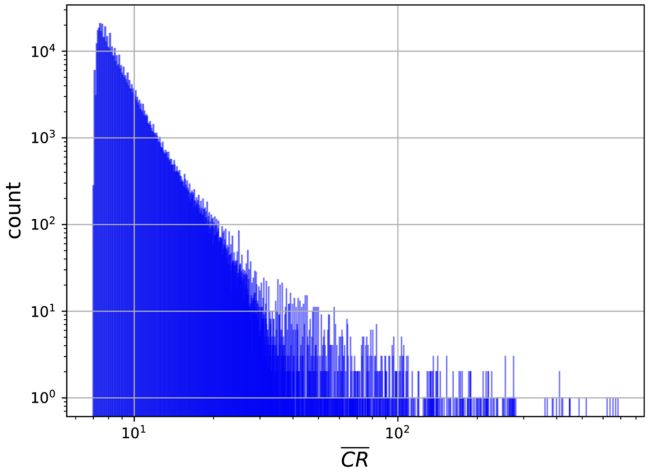

FIG. 5. The critical ratios of coincident candidates returned in our search whose $\overline{CR} > CR_{\rm thr} = 7$. Candidates with $CR < CR_{\rm thr}$ are not shown. $\overline{CR}$ is averaged from candidates returned in both H1 and L1, and corresponds to the candidates that we followed up, all of which were vetoed. In order to compute upper limits on distance reach, we use these CRs in Eq. (B1) and apply the Feldman-Cousins procedure [66] that effectively increases CR to ensure 95% confidence-level coverage. In other words, real GW signals would have had to generate CRs above the ones in this figure at a given chirp mass, time, and frequency to have been detected by our search 95% of the time.

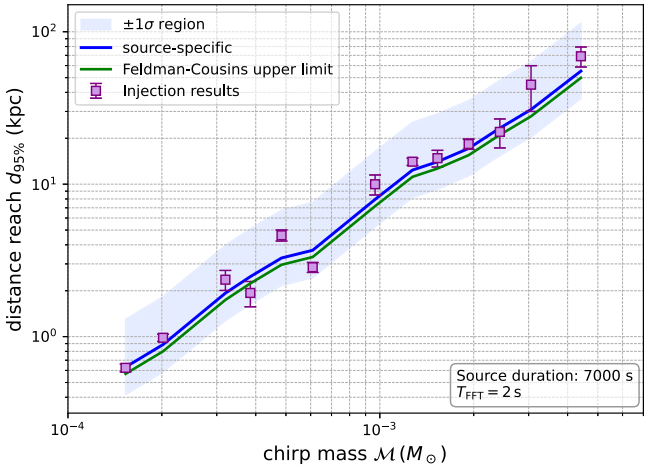

FIG. 6. Comparison of upper limits on distance reach calculated through injections and with the formula given in Eq. (B1). The blue line indicates the theoretical expectation for the distance reach at 95% confidence, adjusted by the source-specific factor $\mathcal{C}$ (see text for details). The shaded region denotes the $\pm 1\sigma$ uncertainty on the distance reach based on the range of source-specific $\mathcal{C}_s$ values. The magenta points indicate the derived distance reach at which 95% of injections are recovered in our simulations. The green line indicates the upper limit that we would actually quote based on the Feldman-Cousins procedure. Our results show that the injection studies agree well with the theoretical blue and green curves and fall well within the shaded region. For each set of 50 injections, at each chirp mass, performed at different distance reaches to derive these results, we analyze different frequency bands and different times across the O4a dataset.

masses in Fig. 6. For each chirp mass, we perform 50 injections over a range of distances away from us, and determine the distance reach at which we recovered at least 95% of injections above $CR_{\rm thr} = 7$ in both detectors. We compare our results to the theoretical distance reach at 95% efficiency given by Eq. (B1). Note that Eq. (B1) represents population-averaged upper limits, therefore, we must specialize this equation to the specific sources we simulate in order to compare them to the sensitivity obtained through injections. In particular, we account for the fact that we have simulated 50 sources with (1) specific choices of inclination and polarization angles, and sky position, and (2) durations that are much less than a sidereal day, both of which affect Eq. (B1). This per-source factor $\mathcal{C}_s$, where s denotes the source number, must be divided out of Eq. (B1) to specialize it to a particular source [108], as discussed previously in the Appendixes of [41,109],

$$\mathcal{C}_s = \sqrt{\frac{\mathcal{S}^2_{\alpha,\delta,\psi,\cos\iota}}{\mathcal{S}^2_t}}, \tag{B4}$$

where

$$\mathcal{S}^2_{\alpha,\delta,\psi,\cos\iota} = \langle (F_+ A_+ + F_\times A_\times)^2 \rangle_{\alpha,\delta,\psi,\cos\iota} \approx \frac{4}{25} \tag{B5}$$

is the factor obtained normally in the derivation of Eq. (B1) by averaging the induced strain over one sidereal day, sky position α, δ, cosine of the inclination angle $\cos\iota$, and the polarization angle ψ. Additionally, A_+ and $A_\times$ are the plus and cross polarizations of the GW, given by

$$A_+ = \frac{1 + \cos^2\iota}{2}, \tag{B6}$$

$$A_\times = \cos\iota. \tag{B7}$$

The factor $\mathcal{S}^2_t$ is obtained at the specific parameters of the source,

$$\mathcal{S}^2_t = \langle F^2_+ \rangle_t A^2_+ + \langle F^2_\times \rangle_t A^2_\times, \tag{B8}$$

where ψ has been averaged out, and the average over time t is taken only over the duration of the source, and

$$F_+(t) = a(t)\cos 2\psi + b(t)\sin 2\psi, \tag{B9}$$

$$F_\times(t) = b(t)\cos 2\psi - a(t)\sin 2\psi \tag{B10}$$

are the time-varying beam pattern functions. The functions $a(t)$ and $b(t)$ are given in [110].

We calculate $\mathcal{C} = \text{mean}(\mathcal{C}_s)$ as an average over the 50 source-specific factors $\mathcal{C}_s$, and then divide Eq. (B1) by $\mathcal{C}$ to plot the dark blue curve in Fig. 6. Furthermore, we shade the $\pm 1\sigma$ around the dark blue curve, which encapsulates the range of possible $\mathcal{C}$, i.e., $\sigma = \text{std}(\mathcal{C}_s)$. Finally, the upper limits that we quote in Fig. 1 rely on the application of the Feldman-Cousins procedure, so we reevaluate the theoretical curve at $CR_{\rm FC} = FC(CR_{\rm thr} = 7) = 8.96$ for comparison. We see that the injections lie comfortably within the shaded area and are consistent with both the source-specific theoretical curve and the Feldman-Cousins curve.

APPENDIX C: OBTAINING RATE DENSITY UPPER LIMITS

For a fixed chirp mass and frequency range, the only parameter that affects the efficiency of the search is the GW amplitude—or, equivalently, the source distance—from the interferometers, so the spacetime volume $\langle VT\rangle$ to which we are sensitive can be written as

$$\langle VT\rangle = T_{\rm obs}\int_0^\infty 4\pi r^2\,\epsilon(r)dr, \tag{C1}$$

where r is an arbitrary distance and $\epsilon(r)$ is the efficiency curve, given by Eq. (8). To compute $\langle VT\rangle$, we can use Laplace's method, which allows us to solve this integral analytically by considering its asymptotic behavior. We define

$$x \equiv \frac{CR_{\rm thr} - (\frac{D}{r})^2}{\sqrt{2}}, \tag{C2}$$

where D is given by Eq. (7) and $CR_{\rm thr} = 7$ is the threshold on the critical ratio that we use to determine which candidates to follow up, and expand linearly around $r_\star = D/\sqrt{CR_{\rm thr}}$, which is the point at which $x = 0$,

$$\begin{aligned} x(r) &\simeq x(r = r_\star) + \left.\frac{dx}{dr}\right|_{r=r_\star}(r - r_\star), \\ &\simeq \frac{\sqrt{2}CR_{\rm thr}^{3/2}}{D}(r - r_\star), \end{aligned} \tag{C3}$$

and thus

$$\epsilon(r) \simeq \frac{1}{2}\text{erfc}\left(\frac{\sqrt{2}CR_{\rm thr}}{D}(r - r_\star)\right). \tag{C4}$$

To leading order, we can replace $\epsilon(r)$ by a step function at the transition point $r_\star$, where the inverse error function erfc starts to rapidly decrease for values $r > r_\star$,

$$\langle VT\rangle \simeq T_{\rm obs}\int_0^{r_\star} 4\pi r^2\,dr, \tag{C5}$$

$$\simeq T_{\rm obs}\frac{4}{3}\pi\left(\frac{D}{\sqrt{CR_{\rm thr}}}\right)^3. \tag{C6}$$

Suppose that we would like to check what the next-to-leading correction would be, to ensure that it is small with respect to what we quote in Eq. (9). To do this, we can change variables such that $u = a(r - r_\star)$, where $a = \frac{\sqrt{2}CR_{\rm thr}^{3/2}}{D}$, and write the integral as

$$\begin{aligned} \langle VT\rangle &= T_{\rm obs}4\pi\int_0^\infty \epsilon(r)r^2dr \\ &\approx T_{\rm obs}4\pi\frac{1}{a}\int_{-ar_\star}^\infty \frac{1}{2}\text{erfc}(u)\left(r_\star + \frac{u}{a}\right)^2 du. \end{aligned} \tag{C7}$$

Splitting $\text{erfc}(u)$ into a step function piece and a correction piece,

$$\frac{1}{2}\text{erfc}(u) = H(-u) + s(u), \tag{C8}$$

where

$$s(u) \equiv \frac{1}{2}(\text{erfc}(u) - 2H(-u)) = \begin{cases} \frac{1}{2}(\text{erfc}(u) - 2), & u < 0, \\ \frac{1}{2}\text{erfc}(u), & u > 0, \end{cases} \tag{C9}$$

and noting that $s(u)$ has the following properties:

$$\int_{-\infty}^\infty s(u)du = 0, \qquad \int_{-\infty}^\infty us(u)du = \frac{1}{4}, \tag{C10}$$

we can calculate the next-to-leading-order piece of $\langle VT\rangle$,

$$\Delta\langle VT\rangle = 4\pi T_{\rm obs}\frac{1}{a}\int_{-\infty}^\infty \frac{1}{2}s(u)\left(r_\star + \frac{u}{a}\right)^2 du. \tag{C11}$$

Here, we have extended the lower bound from $-ar_\star$ to $-\infty$ because the integral takes on the largest values around $r = r_\star$ Using Eq. (C10) and dropping the u^2 term, we arrive at

$$\begin{aligned} \Delta\langle VT\rangle &= 4\pi T_{\rm obs}\frac{r_\star}{2a^2}, \\ &= 4\pi T_{\rm obs}\frac{D^3}{4CR_{\rm thr}^{7/2}}. \end{aligned} \tag{C12}$$

Finally, we can express the leading- and next-to-leading-order contributions as

$$\begin{aligned} \langle VT\rangle_{\rm tot} &\simeq \langle VT\rangle + \Delta\langle VT\rangle \\ &\simeq T_{\rm obs}\frac{4}{3}\pi\left(\frac{D}{\sqrt{CR_{\rm thr}}}\right)^3\left[1 + \frac{3}{4CR_{\rm thr}^2} + \ldots\right]. \end{aligned} \tag{C13}$$

Given that we use $CR_{\rm thr} = 7$ in this paper, the next-to-leading-order term is of $\mathcal{O}(10^{-2})$ and can thus be neglected, allowing us to safely set $\langle VT\rangle_{\rm tot} = \langle VT\rangle$.

From $\langle VT\rangle$, we can compute the rate density constraint by assuming that the event rate for inspiraling planetary-mass ultracompact objects follows a Poissonian distribution, which is consistent with our expectations of how binary black hole objects inspiral and merge. The rate density equation can be derived independently of GW data analysis: we only need to consider inspirals as a Poisson process with a mean number of expected events of $\lambda = \mathcal{R}\langle VT\rangle$. In a Poisson process, the probability that we observe zero events N is

$$P(N = 0|\lambda) = e^{-\lambda}. \tag{C14}$$

To obtain an upper limit at a given confidence level α, we simply need to set

$$P(N = 0|\lambda) = 1 - \alpha = e^{-\lambda}. \tag{C15}$$

By setting $\alpha = 0.9$ and solving for $\mathcal{R}$, we obtain Eq. (10).

APPENDIX D: FROM COSMOLOGICAL TO GALACTIC RATES

In this Appendix, we describe the methodology to obtain galactic merger rates as a function of the distance reach D outputted by the search. The expected rate is obtained from the cosmological merger rate densities, multiplied by the probe volume $\frac{4}{3}\pi D^3$ and by the ratio between the averaged DM density in this volume and the cosmological density. We use a standard Navarro-Frenk-White profile,

$$\rho(r) = \frac{\rho_0}{\frac{r}{R_{\rm s}}(1+\frac{r}{R_{\rm s}})^2}, \tag{D1}$$

with $R_{\rm s} = 21.5$ kpc and $\rho_0 = 8\times 10^6 M_\odot\,{\rm kpc}^{-3}$. Using another type of profile, such as an Einasto profile, only changes our results marginally. The enclosed DM mass $M_{\rm DM}(D)$ is obtained by integrating the profile centered on the Sun's location, at $R_\odot = 8.2$ kpc from the Galactic Center, to get

$$M_{\rm DM}(D) = 2\pi\int_0^\pi\int_0^D r^2\rho\left(\sqrt{r^2+R_\odot^2-2rR_\odot\cos(\phi)}\right) \times \sin(\phi){\rm d}r{\rm d}\phi. \tag{D2}$$

We then compute the factor $F(d)$ as the ratio between the averaged density at distance d and the density at the Sun's location. The obtained value of $F(d)$ is shown in Fig. 7. As expected, it is close to one for short distances compared to the galaxy scale. It shows a slight peak at $d\sim 8$ kpc that corresponds to the distance of the Galactic Center where DM density is strongly enhanced. But we note that the rate enhancement is small because the search is sensitive to all directions of the sky and not only the Galactic Center. At larger distances, $F(d)$ decreases, and above 50 kpc, it decreases like $1/d^3$, as expected given that the DM density decays and the total mass probed does not vary much. We then obtain a constant rate value compatible with the one calculated in [30], $R^{\rm gal} \approx 2\times 10^{-8}\times \mathcal{R}^{\rm prim}_{\rm cos}$ Gpc^3.

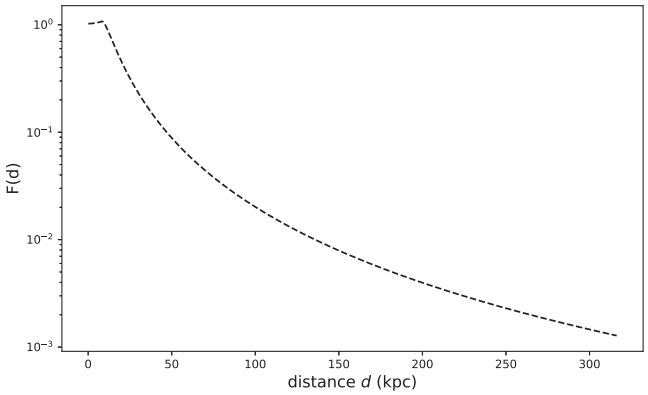

FIG. 7. How the factor $F(d)$ falls off as as a function of distance from Earth. $F(d)$ encodes the ratio of the averaged DM density at a distance d compared to that at the Sun's position.

APPENDIX E: EVALUATING ROBUSTNESS OF CONSTRAINTS

1. Eccentricity

Our constraints have implicitly assumed that GWs from inspiraling compact objects follow the time-frequency evolution $f_{3.5PN}(t)$. It is, however, worth discussing whether additional physics could affect our ability to set upper limits on PBHs. We consider to what extent binary eccentricity would alter our conclusions. Early-Universe PBHs have merger timescales of the order of the age of the Universe, therefore, they are expected to radiate away their eccentricity by the time that they enter the LIGO, Virgo, and KAGRA frequency band [111–113]. However, PBH binaries formed by dynamical capture due to GW braking in DM halos in the late Universe would retain some eccentricity, depending on the velocity dispersion and the halo mass, with higher relative velocities (that result from larger halo masses) leading to tighter binaries and larger eccentricities [114,115]. Therefore, the detection of eccentricity could indicate a particular type of binary formation.

To demonstrate our sensitivity to eccentric systems, we require that the frequency shift induced by eccentricity would be confined to one frequency bin for the total signal duration. In other words, we cannot distinguish between $f_{3.5PN}(t)$ and the signal time-frequency evolution with eccentricity. The key quantity here is the time-frequency track: eccentricity does not cause frequency fluctuations throughout the signal's time-frequency track by more than

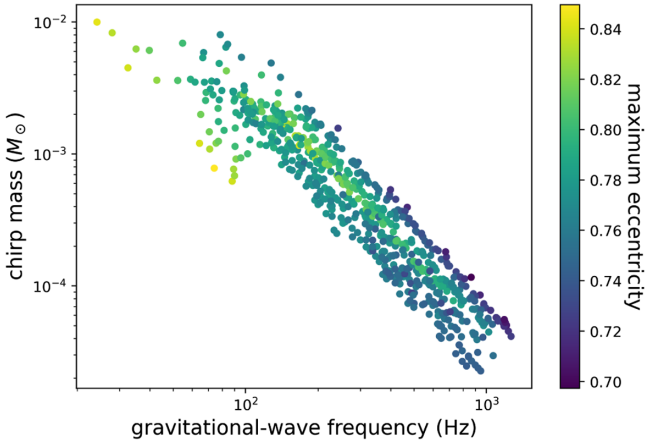

FIG. 8. The median maximum eccentricity that each configuration in our search could probe. We show that, for asymmetric mass-ratio systems, we can be sensitive to eccentricities as high as 0.84, depending on the GW frequency and chirp mass of the system.

one frequency bin. In other words, if [42,43]

$$\dot{f}_{\rm GW} g(e) T_{\rm FFT} \leq \frac{1}{T_{\rm FFT}} \tag{E1}$$

we would not miss eccentric systems. The function that characterizes the eccentricity e is given by [43]

$$g(e) = (1-e^2)^{-7/2}\left(1 + \frac{73}{24}e^2 + \frac{37}{96}e^4\right). \tag{E2}$$

Plugging Eq. (1) into Eq. (E1) and solving for $g(e)$, we obtain

$$g(e) \lesssim 8000\left(\frac{1\ \text{s}}{T_{\rm FFT}}\right)^2\left(\frac{10^{-3}M_\odot}{\mathcal{M}}\right)^{5/3}\left(\frac{100\ \text{Hz}}{f_{\rm GW}}\right)^{11/3}. \tag{E3}$$

Solving for the eccentricity is analytically unfeasible, so we numerically compute the maximum eccentricity $e_{\rm max}$ to which each configuration is sensitive. Given that each configuration covers a wide range of $f_{\rm GW}$ and $\mathcal{M}$, we calculate the median $e_{\rm max}$ by sampling over the range of $f_{\rm GW}, \mathcal{M}$ each configuration could detect. We plot these median $e_{\rm max}$ in Fig. 8. For comparison, a pessimistic evaluation of Eq. (E3) using the maximum frequency and chirp mass in each configuration results in a sensitivity to binaries with maximum eccentricities of [0.33, 0.72], with a median of 0.46. On the other hand, an optimistic evaluation using the minimum frequency and chirp mass probed in each configuration would permit us to detect binaries with eccentricities between [0.86, 0.97], with a median of 0.91.

2. Conditions on the PBH mass distribution

Calculating PBH merger rates is highly model dependent. In particular, the choice of the PBH mass distribution can significantly affect the predicted suppression of merger rates. This suppression mainly arises from the disruption of binaries, either through early interactions with intruding PBHs or via late encounters with other PBHs within clusters formed by Poisson fluctuations. Some sufficient conditions to avoid such a suppression have been identified, and in this Appendix we provide a more detailed explanation for these conditions, based on the current prescriptions for the merger rates.

a. Early perturbers

The first two conditions ensure that most binaries are not gravitationally bound to their neighbors when forming. Assuming $f_{\rm PBH} \gg \sigma_{\rm M}$ (where $\sigma_{\rm M}^2$ is the variance of matter density perturbations at the time the binary forms), the suppression factor associated with the early disruption of binaries by a nearby intruder can be expressed as [71,72,116]

$$f_{\rm sup}^{\rm (dist)} \approx 1.42\left(\frac{\langle m^2\rangle/\langle m\rangle^2}{\bar{N}(y)+0.4}\right)^{-21/74}\exp(-\bar{N}), \tag{E4}$$

where $\bar{N}$ is the expected number of PBHs within the binary's sphere of influence at scale factor a, given by

$$\bar{N} = \frac{M}{\langle m\rangle}\frac{f_{\rm PBH}}{f_{\rm PBH}+a_{\rm eq}/a}, \tag{E5}$$

with M denoting the total mass of the binary, $\langle m\rangle = \rho_{\rm PBH}/n_{\rm PBH}$ the average PBH mass, and $a_{\rm eq}$ the scale factor at matter-radiation equality. Since the number density of PBHs, $n_{\rm PBH}$, scales inversely with mass, lighter PBHs can significantly outnumber the PBHs from the peak, even with a subdominant contribution to the total PBH energy density, increasing $\bar{N}$ and driving the suppression factor toward zero. Consequently, only mass functions with a suppressed low-mass tail can survive such heavy disruption. In these cases, for symmetric binaries, one typically finds $\bar{N} \approx 2$ yielding a suppression factor of $f_{\rm sup} \approx 0.2$. For asymmetric binaries, $M \approx m_1$ such that $\bar{N} \approx 1$, which yield a suppression factor of $f_{\rm sup} \approx 0.5$. These are the two cases we consider to produce Fig. 4.

b. Late perturbers

One additional condition that must be fulfilled in all scenarios is to avoid the rate suppression due to the interactions of the binaries with PBHs inside clusters seeded by Poisson fluctuations. The standard prescription, validated by numerical simulations for peaked distributions, leads to a rate suppression factor today approximately given by

$$f_{\rm sup}^{\rm (cl)} \approx 0.01 f_{\rm PBH}^{-0.65} \tag{E6}$$

when a significant DM fraction is made of PBHs, i.e., an additional suppression by up to 2 orders of magnitude. However, we can show that such a suppression can be avoided for low-mass PBHs. From Ref. [71], binaries are perturbed by encounters with PBHs of mass m_3 inside clusters when the impact parameter is

$$b \lesssim \frac{[m_3(m_1+m_2+m_3)]^{1/3} r_a^{1/2}}{j_\tau^{1/3}(m_1+m_2)^{1/6} v_{\rm rel}}, \tag{E7}$$

where r_a is the separation and j_τ the angular momentum of the binary, expected to merge today, for which estimations are provided in Ref. [71],

$$j_\tau = 1.7\times 10^{-2}\left(\frac{m_1+m_2}{M_\odot}\right)^{5/37}\frac{(4m_1m_2)^{3/37}}{(m_1+m_2)^{6/37}} f_{\rm PBH}^{16/37} \tag{E8}$$

and

$$r_a = 2.13\times 10^9 \text{ m}\times\left[\frac{m_1m_2(m_1+m_2)}{M_\odot^3}\right]^{1/4}, \tag{E9}$$

and where $v_{\rm rel}$ is the relative velocity, of the same order as the virial velocity of the cluster. The corresponding interaction cross section is then given by $\sigma=\pi b^2$ and one can then estimate, for each PBH mass m_3 with an abundance characterized by $f(\ln m_3)$, the typical time it takes to perturb the binary, $t_{\rm pert}=1/[n(m_3)\sigma v_{\rm rel}]$, where $n(m_3)$ is the number density of perturbers of mass m_3 in the cluster. For a wide mass distribution, one has to integrate $n(m_3)\sigma v_{\rm rel}$ over the full distribution to get the total perturbation rate. For simplicity, we only show here that any value of m_3 gives rise to $t_{\rm pert}\gg t_0$, the age of the Universe, with some conditions on the PBH clusters. But in general, $t_{\rm pert}$ depend on the typical clustering scale. From Ref. [71], this time was found to be typically much smaller than the age of the Universe, leading to automatic binary perturbations in clusters. Nevertheless, the clustering process is complex and is also impacted by the dynamical heating of small clusters and their dilution in larger clusters. As explained in [117], if there exist a mass range m in the distribution for which one has $f(m)m/M_\odot\sim\mathcal{O}(1)$, then the smallest clusters will have a radius of order 20 parsecs and a mass around $10^6 M_\odot$ that could be associated to ultrafaint dwarf galaxies, a larger value of that combination being excluded by the observations of these ultrafaint dwarfs. These clusters would have virial velocities of order of a few km/s. We have calculated the interaction time needed to perturb binaries with component masses m_1 and m_2 as

$$\begin{aligned} t_{\rm pert} \approx{}& 2.7\times 10^{10}\text{ yr}\times f_{\rm PBH}^{-79/111} f(\ln m_3)^{-1} \\ &\times\left(\frac{m_1m_2}{M_\odot^2}\right)^{-\frac{29}{148}}\left(\frac{m_3}{M_\odot}\right)^{\frac{1}{3}}\left(\frac{m_1+m_2}{M_\odot}\right)^{\frac{29}{144}} \\ &\times\left(\frac{m_1+m_2+m_3}{M_\odot}\right)^{-\frac{2}{3}}\left(\frac{M_{\rm cl}}{M_\odot}\right)^{-\frac{1}{2}}\left(\frac{r_{\rm cl}}{\rm pc}\right)^{5/2}, \end{aligned} \tag{E10}$$

where $M_{\rm cl}$ and $r_{\rm cl}$ are the cluster mass and radius, respectively. Taking $f(\ln m_3)=1$, for the typical above-mentioned clusters and the relevant masses and values of $f_{\rm PBH}$ for this work, this time is found to exceed the age of the Universe, lower abundances leading obviously to even larger interaction times. But let us note again the importance of the large cluster mass compared to what was considered in [71,116]. A heavy-mass tail in the distribution, or a high peak at the solar-mass scale with a significant $f_{\rm PBH}$, are therefore required to prevent merger rates to be suppressed due to PBH clusters.

Finally, let us notice that we have checked that the other PBH binary formation channels, reviewed in [71], namely the 3-body early binary formation channel and the late 2-body and 3-body channels in PBH clusters, generically lead to lower merger rates than for early binaries, for significant values of $f_{\rm PBH}$, both for equal-mass subsolar mergers and for asymmetric binaries. These have therefore not been considered in our analysis.

[1] LIGO Scientific, Virgo and KAGRA Collaborations, O4a PBH CW Data Release, LIGO Document Control Center, LIGO-P2500686-v1 (2025).

[2] B. Abbott *et al.* (LIGO Scientific and Virgo Collaborations), Phys. Rev. Lett. **116**, 061102 (2016).

[3] B. Abbott *et al.* (LIGO Scientific and Virgo Collaborations), Phys. Rev. X **6**, 041015 (2016); **8**, 039903(E) (2018).

[4] B. P. Abbott *et al.* (LIGO Scientific and Virgo Collaborations), Phys. Rev. Lett. **116**, 241103 (2016).

[5] B. P. Abbott *et al.* (LIGO Scientific and Virgo Collaborations), Phys. Rev. Lett. **118**, 221101 (2017); **121**, 129901 (E) (2018).

[6] B. P. Abbott *et al.* (LVC Collaboration), Phys. Rev. Lett. **119**, 141101 (2017).

[7] B. P. Abbott *et al.* (LIGO Scientific and Virgo Collaborations), Astrophys. J. **851**, L35 (2017).
[8] B. P. Abbott *et al.* (LIGO Scientific and Virgo Collaborations), Phys. Rev. X **9**, 031040 (2019).
[9] R. Abbott *et al.* (LIGO Scientific and Virgo Collaborations), Phys. Rev. D **102**, 043015 (2020).
[10] B. Abbott *et al.* (LIGO Scientific and Virgo Collaborations), Astrophys. J. Lett. **892**, L3 (2020).
[11] R. Abbott *et al.* (LIGO Scientific and Virgo Collaborations), Astrophys. J. **896**, L44 (2020).
[12] R. Abbott *et al.* (LIGO Scientific and Virgo Collaborations), Phys. Rev. Lett. **125**, 101102 (2020).
[13] R. Abbott *et al.* (LIGO Scientific and Virgo Collaborations), Astrophys. J. **900**, L13 (2020).
[14] A. G. Abac *et al.* (LIGO Scientific, Virgo, and KAGRA Collaborations), Astrophys. J. Lett. **970**, L34 (2024).
[15] R. Abbott *et al.* (LIGO Scientific and Virgo Collaborations), Phys. Rev. Lett. **125**, 101102 (2020).
[16] R. Abbott *et al.* (LIGO Scientific and Virgo Collaborations), Phys. Rev. X **11**, 021053 (2021).
[17] R. Abbott *et al.* (LIGO Scientific, Virgo, and KAGRA Collaborations), Phys. Rev. X **13**, 041039 (2023).
[18] S. Hawking, Mon. Not. R. Astron. Soc. **152**, 75 (1971).
[19] B. Carr, S. Clesse, J. García-Bellido, and F. Kühnel, Phys. Dark Universe **31**, 100755 (2021).
[20] S. Bird, I. Cholis, J. B. Muñoz, Y. Ali-Haïmoud, M. Kamionkowski, E. D. Kovetz, A. Raccanelli, and A. G. Riess, Phys. Rev. Lett. **116**, 201301 (2016).
[21] S. Clesse and J. García-Bellido, Phys. Dark Universe **15**, 142 (2017).
[22] M. Sasaki, T. Suyama, T. Tanaka, and S. Yokoyama, Phys. Rev. Lett. **117**, 061101 (2016); **121**, 059901(E) (2018).
[23] B. P. Abbott *et al.* (LIGO Scientific and Virgo Collaborations), Phys. Rev. Lett. **123**, 161102 (2019).
[24] R. Abbott *et al.* (LIGO Scientific, Virgo, and KAGRA Collaborations), Phys. Rev. Lett. **129**, 061104 (2022).
[25] K. S. Phukon, G. Baltus, S. Caudill, S. Clesse, A. Depasse, M. Fays, H. Fong, S. J. Kapadia, R. Magee, and A. J. Tanasijczuk, arXiv:2105.11449.
[26] A. H. Nitz and Y.-F. Wang, Phys. Rev. Lett. **127**, 151101 (2021).
[27] A. H. Nitz and Y.-F. Wang, Astrophys. J. **915**, 54 (2021).
[28] R. Abbott *et al.* (LIGO Scientific, Virgo, and KAGRA Collaborations), Mon. Not. R. Astron. Soc. **524**, 5984 (2023); **526**, 6234(E) (2023).
[29] A. H. Nitz and Y.-F. Wang, Phys. Rev. D **106**, 023024 (2022).
[30] A. L. Miller, S. Clesse, F. De Lillo, G. Bruno, A. Depasse, and A. Tanasijczuk, Phys. Dark Universe **32**, 100836 (2021).
[31] M. Andrés-Carcasona, O. J. Piccinni, M. Martínez, and L.-M. Mir, Proc. Sci.EPS-HEP2023 (**2024**) 067.
[32] G. Alestas, G. Morras, T. S. Yamamoto, J. Garcia-Bellido, S. Kuroyanagi, and S. Nesseris, Phys. Rev. D **109**, 123516 (2024).
[33] M. Andrés-Carcasona, O. J. Piccinni, M. Martínez, and L. M. Mir, Phys. Rev. D **111**, 043019 (2025).
[34] A. L. Miller, N. Aggarwal, S. Clesse, F. De Lillo, S. Sachdev, P. Astone, C. Palomba, O. J. Piccinni, and L. Pierini, Phys. Rev. D **110**, 082004 (2024).
[35] A. L. Miller, Gravitational waves from sub-solar mass primordial black holes, in *Primordial Black Holes*, edited by C. Byrnes, G. Franciolini, T. Harada, P. Pani, and M. Sasaki (Springer Nature Singapore, Singapore, 2025), pp. 467–494.
[36] A. L. Miller, N. Aggarwal, S. Clesse, F. De Lillo, S. Sachdev, P. Astone, C. Palomba, O. J. Piccinni, and L. Pierini, Phys. Rev. Lett. **133**, 111401 (2024).
[37] J. Aasi, B. P. Abbott, R. Abbott, T. Abbott, M. R. Abernathy, K. Ackley, C. Adams, T. Adams, P. Addesso *et al.*, Classical Quantum Gravity **32**, 074001 (2015).
[38] F. Acernese, M. Agathos, K. Agatsuma, D. Aisa, N. Allemandou, A. Allocca, J. Amarni, P. Astone, G. Balestri, and G. Ballardin *et al.*, Classical Quantum Gravity **32**, 024001 (2015).
[39] T. Akutsu *et al.* (KAGRA Collaboration), Prog. Theor. Exp. Phys. **2021**, 05A101 (2021).
[40] A. L. Miller, N. Aggarwal, S. Clesse, and F. De Lillo, Phys. Rev. D **105**, 062008 (2022).
[41] R. Abbott *et al.* (LIGO Scientific, Virgo, and KAGRA Collaborations), Phys. Rev. D **106**, 102008 (2022).
[42] A. L. Miller, Phys. Rev. D **112**, 103027 (2025).
[43] M. Maggiore, *Gravitational Waves: Volume 1: Theory and Experiments* (Oxford University Press, New York, 2008), Vol. 1.
[44] R. Prix, S. Giampanis, and C. Messenger, Phys. Rev. D **84**, 023007 (2011).
[45] K. Riles, Living Rev. Relativity **26**, 3 (2023).
[46] A. G. Abac *et al.*, arXiv:2603.14168.
[47] S. Soni *et al.* (LIGO Collaboration), Classical Quantum Gravity **42**, 085016 (2025).
[48] D. Ganapathy *et al.* (LIGO O4 Detector Collaboration), Phys. Rev. X **13**, 041021 (2023).
[49] W. Jia *et al.* (members of the LIGO Scientific† Collaboration), Science **385**, 1318 (2024).
[50] E. Capote *et al.*, Phys. Rev. D **111**, 062002 (2025).
[51] S. Karki *et al.*, Rev. Sci. Instrum. **87**, 114503 (2016).
[52] A. Viets *et al.*, Classical Quantum Gravity **35**, 095015 (2018).
[53] M. Wade *et al.*, Classical Quantum Gravity **42**, 215016 (2025).
[54] E. Goetz and K. Riles, Segments used for creating standard SFTs in O4 data, Technical Note LIGO-T2400058-v1 (LIGO Laboratory, 2025) version v1; other version: LIGO-T2400058-v2, https://dcc.ligo.org/T2400058-v1/public.
[55] P. Astone, S. Frasca, and C. Palomba, Classical Quantum Gravity **22**, S1197 (2005).
[56] P. Astone and S. D'Antonio, Creation of the short FFT data base (SFDB) (2025), 10.15161/oar.it/tqwgf-nq452.
[57] A. Miller *et al.*, Phys. Rev. D **98**, 102004 (2018).
[58] S. S. Menon *et al.*, arXiv:2512.09878.
[59] L. Pierini, Generalized frequency hough (gfh-v2). new core function developed under ICSC (2025), 10.15161/oar.it/35swc-fes27, software for computing the Generalized Frequency Hough transform used in long-duration gravitational wave searches.
[60] A. L. Miller (LIGO Scientific, Virgo, and KAGRA Collaborations), Codes to perform the o4a search for ultra-compact planetary-mass binaries, 10.5281/zenodo.17984228 (2025).
[61] E. Goetz *et al.*, O4a lines and combs found in self-gated C00 cleaned data, Technical Note LIGO-T2400204-v2 (LIGO Laboratory, 2024), version v2.

[62] P. Astone, A. Colla, S. D'Antonio, S. Frasca, and C. Palomba, Phys. Rev. D **90**, 042002 (2014).
[63] O. J. Piccinni, P. Astone, S. D'Antonio, S. Frasca, G. Intini, P. Leaci, S. Mastrogiovanni, A. Miller, C. Palomba, and A. Singhal, Classical Quantum Gravity **36**, 015008 (2019).
[64] P. Astone, L. Pierini, L. Silvestri, S. D. Pra, and C. Palomba, Example frequency hough (2025), https://www.openaccessrepository.it/doi/10.15161/oar.it/35swc-fes27.
[65] A. L. Miller, Using machine learning and the hough transform to search for gravitational waves from young isolated neutron stars, Ph.D. thesis, University of Florida, 2020, https://ufdc.ufl.edu/UFE0055970/00001.
[66] G. J. Feldman and R. D. Cousins, Phys. Rev. D **57**, 3873 (1998).
[67] B. P. Abbott *et al.* (LIGO Scientific and Virgo Collaborations), Astrophys. J. **875**, 160 (2019).
[68] P. R. Brady, J. D. E. Creighton, and A. G. Wiseman, Classical Quantum Gravity **21**, S1775 (2004).
[69] S. Fairhurst and P. Brady, Classical Quantum Gravity **25**, 105002 (2008).
[70] R. Biswas, P. R. Brady, J. D. E. Creighton, and S. Fairhurst, Classical Quantum Gravity **26**, 175009 (2009); **30**, 079502 (E) (2013).
[71] M. Raidal, V. Vaskonen, and H. Veermäe, Formation of primordial black hole binaries and their merger rates, in *Primordial Black Holes*, edited by C. Byrnes, G. Franciolini, T. Harada, P. Pani, and M. Sasaki (Springer, Singapore, 2025).
[72] M. Raidal, C. Spethmann, V. Vaskonen, and H. Veermäe, J. Cosmol. Astropart. Phys. 02 (2019) 018.
[73] M. Weber and W. de Boer, Astron. Astrophys. **509**, A25 (2010).
[74] C. T. Byrnes, M. Hindmarsh, S. Young, and M. R. S. Hawkins, J. Cosmol. Astropart. Phys. 08 (2018) 041.
[75] B. J. Kavanagh, D. Gaggero, and G. Bertone, Phys. Rev. D **98**, 023536 (2018).
[76] R. Abbott *et al.* (LVK Collaboration), Mon. Not. R. Astron. Soc. **524**, 5984 (2023); **526**, 6234(E) (2023).
[77] Y.-F. Wang and A. H. Nitz, Mon. Not. R. Astron. Soc. **528**, 3891 (2024).
[78] T. Boybeyi, S. Clesse, S. Kuroyanagi, and M. Sakellariadou, Phys. Rev. D **112**, 023551 (2025).
[79] A. G. Abac *et al.* (The LIGO Scientific, Virgo, and KAGRA Collaborations), arXiv:2510.26848.
[80] P. Tisserand *et al.* (EROS-2 Collaboration), Astron. Astrophys. **469**, 387 (2007).
[81] D. Croon, D. McKeen, N. Raj, and Z. Wang, Phys. Rev. D **102**, 083021 (2020).
[82] P. Mróz *et al.*, Astrophys. J. Lett. **976**, L19 (2024).
[83] P. Mróz *et al.*, Nature (London) **632**, 749 (2024).
[84] M. Gorton and A. M. Green, J. Cosmol. Astropart. Phys. 08 (2022) 035.
[85] A. M. Green, J. Cosmol. Astropart. Phys. 04 (2025) 023.
[86] J. Garcia-Bellido and M. Hawkins, Universe **10**, 449 (2024).
[87] B. J. Kavanagh, bradkav/pbhbounds: Release version (2019), 10.5281/zenodo.3538999.
[88] A. L. Miller, cw_constrain: Constraining PBH abundance and the GeV excess with continuous gravitational waves (2025), 10.5281/zenodo.15559328.
[89] A. L. Miller, pyhough: Searches for continuous gravitational waves with the hough transform (2025), 10.5281/zenodo.15512455.
[90] A. Ramos-Buades, A. Buonanno, M. Khalil, and S. Ossokine, Phys. Rev. D **105**, 044035 (2022).
[91] X. Liu, Z. Cao, and Z.-H. Zhu, Classical Quantum Gravity **41**, 195019 (2024).
[92] R. Gamba, D. Chiaramello, and S. Neogi, Phys. Rev. D **110**, 024031 (2024).
[93] A. Nagar, R. Gamba, P. Rettegno, V. Fantini, and S. Bernuzzi, Phys. Rev. D **110**, 084001 (2024).
[94] A. Gamboa *et al.*, Phys. Rev. D **112**, 044038 (2025).
[95] S. Bhaumik *et al.*, Phys. Rev. D **111**, 123032 (2025).
[96] G. Morras, G. Pratten, and P. Schmidt, Astrophys. J. Lett. **1000**, L2 (2026).
[97] G. Morras, G. Pratten, and P. Schmidt, Phys. Rev. D **111**, 084052 (2025).
[98] M. d. L. Planas, A. Ramos-Buades, C. García-Quirós, H. Estellés, S. Husa, and M. Haney, Phys. Rev. D **113**, 024006 (2026).
[99] G. Huez, S. Bernuzzi, M. Breschi, and R. Gamba, Phys. Rev. D **112**, 084054 (2025).
[100] G. Bertone *et al.*, SciPost Phys. Core **3**, 007 (2020).
[101] B. J. Kavanagh, D. A. Nichols, G. Bertone, and D. Gaggero, Phys. Rev. D **102**, 083006 (2020).
[102] P. S. Cole, G. Bertone, A. Coogan, D. Gaggero, T. Karydas, B. J. Kavanagh, T. F. M. Spieksma, and G. M. Tomaselli, Nat. Astron. **7**, 943 (2023).
[103] B. J. Kavanagh, T. K. Karydas, G. Bertone, P. Di Cintio, and M. Pasquato, Phys. Rev. D **111**, 063071 (2025).
[104] T. K. Karydas, B. J. Kavanagh, and G. Bertone, Phys. Rev. D **111**, 063070 (2025).
[105] C. Dyson, T. F. M. Spieksma, R. Brito, M. van de Meent, and S. Dolan, Phys. Rev. Lett. **134**, 211403 (2025).
[106] S. Mitra, N. Speeney, S. Chakraborty, and E. Berti, Phys. Rev. D **112**, 044030 (2025).
[107] https://dcc.ligo.org/LIGO-M2300033/public.
[108] C. Palomba, On the sensitivity of peakmap-based methods for the search of continuous gravitational wave signals, Scientific & Technical Note VIR-0724B-25 (Virgo Collaboration, 2025), https://tds.virgo-gw.eu/?r=25138.
[109] A. L. Miller and Y. Zhao, Phys. Rev. Lett. **131**, 081401 (2023).
[110] P. Jaranowski, A. Krolak, and B. F. Schutz, Phys. Rev. D **58**, 063001 (1998).
[111] I. Musco and J. C. Miller, Classical Quantum Gravity **30**, 145009 (2013).
[112] T. Nakamura, M. Sasaki, T. Tanaka, and K. S. Thorne, Astrophys. J. Lett. **487**, L139 (1997).
[113] K. Ioka, T. Chiba, T. Tanaka, and T. Nakamura, Phys. Rev. D **58**, 063003 (1998).
[114] I. Cholis, E. D. Kovetz, Y. Ali-Haïmoud, S. Bird, M. Kamionkowski, J. B. Muñoz, and A. Raccanelli, Phys. Rev. D **94**, 084013 (2016).
[115] Y.-F. Wang and A. H. Nitz, Astrophys. J. **912**, 53 (2021).
[116] G. Hütsi, M. Raidal, V. Vaskonen, and H. Veermäe, J. Cosmol. Astropart. Phys. 03 (2021) 068.
[117] B. Carr, S. Clesse, J. Garcia-Bellido, M. Hawkins, and F. Kuhnel, Phys. Rep. **1054**, 1 (2024).

A. G. Abac,[1] I. Abouelfettouh,[2] F. Acernese,[3,4] K. Ackley,[5] C. Adamcewicz,[6] S. Adhicary,[7] D. Adhikari,[8,9] N. Adhikari,[10] R. X. Adhikari,[11] V. K. Adkins,[12] S. Afroz,[13] A. Agapito,[14] D. Agarwal,[15] M. Agathos,[16] N. Aggarwal,[17] S. Aggarwal,[18] O. D. Aguiar,[19] I.-L. Ahrend,[20] L. Aiello,[21,22] A. Ain,[23] P. Ajith,[24] T. Akutsu,[25,26] S. Albanesi,[27,28] W. Ali,[29,30] S. Al-Kershi,[8,9] C. Alléné,[31] A. Allocca,[32,4] S. Al-Shammari,[33] P. A. Altin,[34] S. Alvarez-Lopez,[35] W. Amar,[31] O. Amarasinghe,[33] A. Amato,[36,37] F. Amicucci,[38,39] C. Amra,[40] A. Ananyeva,[11] S. B. Anderson,[11] W. G. Anderson,[11] M. Andia,[41] M. Ando,[42] M. Andrés-Carcasona,[43] T. Andrić,[44,45,8,9] J. Anglin,[46] S. Ansoldi,[47,48] J. M. Antelis,[49] S. Antier,[41] M. Aoumi,[50] E. Z. Appavuravther,[51,52] S. Appert,[11] S. K. Apple,[53] K. Arai,[11] A. Araya,[42] M. C. Araya,[11] M. Arca Sedda,[44,45] J. S. Areeda,[54] N. Aritomi,[2] F. Armato,[29,30] S. Armstrong,[55] N. Arnaud,[56] M. Arogeti,[57] S. M. Aronson,[12] K. G. Arun,[58] G. Ashton,[59] Y. Aso,[25,60] L. Asprea,[28] M. Assiduo,[61,62] S. Assis de Souza Melo,[63] S. M. Aston,[64] P. Astone,[38] F. Attadio,[39,38] F. Aubin,[65] K. AultONeal,[66] G. Avallone,[67] E. A. Avila,[49] S. Babak,[20] C. Badger,[68] S. Bae,[69] S. Bagnasco,[28] L. Baiotti,[70] R. Bajpai,[71] T. Baka,[72,37] A. M. Baker,[6] K. A. Baker,[73] T. Baker,[74] G. Baldi,[75,76] N. Baldicchi,[77,51] M. Ball,[78] G. Ballardin,[63] S. W. Ballmer,[79] S. Banagiri,[6] B. Banerjee,[44] D. Bankar,[80] T. M. Baptiste,[12] P. Baral,[10] M. Baratti,[81,82] J. C. Barayoga,[11] B. C. Barish,[11] D. Barker,[2] N. Barman,[80] P. Barneo,[83,84,85] F. Barone,[86,4] B. Barr,[87] L. Barsotti,[35] M. Barsuglia,[20] D. Barta,[88] A. M. Bartoletti,[89] M. A. Barton,[87] I. Bartos,[46] A. Basalaev,[8,9] R. Bassiri,[90] A. Basti,[82,81] M. Bawaj,[77,51] P. Baxi,[91] J. C. Bayley,[87] A. C. Baylor,[10] P. A. Baynard II,[57] M. Bazzan,[92,93] V. M. Bedakihale,[94] F. Beirnaert,[95] M. Bejger,[96] D. Belardinelli,[22] A. S. Bell,[87] D. S. Bellie,[97] L. Bellizzi,[81,82] W. Benoit,[18] I. Bentara,[56] J. D. Bentley,[98] M. Ben Yaala,[55] S. Bera,[99,100] F. Bergamin,[33] B. K. Berger,[90] S. Bernuzzi,[27] M. Beroiz,[11] C. P. L. Berry,[87] D. Bersanetti,[29] T. Bertheas,[101] A. Bertolini,[37,36] J. Betzwieser,[64] D. Beveridge,[73] G. Bevilacqua,[102] N. Bevins,[103] R. Bhandare,[104] R. Bhatt,[11] D. Bhattacharjee,[105,106] S. Bhattacharyya,[107] S. Bhaumik,[46] V. Biancalana,[102] A. Bianchi,[37,108] I. A. Bilenko,[109] G. Billingsley,[11] A. Binetti,[110] S. Bini,[11,75,76] C. Binu,[111] S. Biot,[112] O. Birnholtz,[113] S. Biscoveanu,[97] A. Bisht,[9] M. Bitossi,[63,81] M.-A. Bizouard,[114] S. Blaber,[115] J. K. Blackburn,[11] L. A. Blagg,[78] C. D. Blair,[73,64] D. G. Blair,[73] N. Bode,[8,9] N. Boettner,[98] G. Boileau,[114] M. Boldrini,[38] G. N. Bolingbroke,[116] A. Bolliand,[117,40] L. D. Bonavena,[46] R. Bondarescu,[83] F. Bondu,[118] E. Bonilla,[90] M. S. Bonilla,[54] A. Bonino,[119] R. Bonnand,[31,117] A. Borchers,[8,9] V. Boschi,[81] S. Bose,[120] V. Bossilkov,[64] Y. Bothra,[37,108] A. Boudon,[56] L. Bourg,[57] M. Boyle,[121] A. Bozzi,[63] C. Bradaschia,[81] P. R. Brady,[10] A. Branch,[64] M. Branchesi,[44,45] I. Braun,[105] T. Briant,[122] A. Brillet,[114] M. Brinkmann,[8,9] P. Brockill,[10] E. Brockmueller,[8,9] A. F. Brooks,[11] B. C. Brown,[46] D. D. Brown,[116] M. L. Brozzetti,[77,51] S. Brunett,[11] G. Bruno,[15] R. Bruntz,[123] J. Bryant,[119] Y. Bu,[124] F. Bucci,[62] J. Buchanan,[123] O. Bulashenko,[83,84] T. Bulik,[125] H. J. Bulten,[37] A. Buonanno,[126,1] K. Burtnyk,[2] R. Buscicchio,[127,128] D. Buskulic,[31] C. Buy,[101] R. L. Byer,[90] G. S. Cabourn Davies,[74] R. Cabrita,[15] V. Cáceres-Barbosa,[7] L. Cadonati,[57] G. Cagnoli,[129] C. Cahillane,[79] A. Calafat,[99] T. A. Callister,[130] E. Calloni,[32,4] S. R. Callos,[78] M. Canepa,[30,29] G. Caneva Santoro,[43] K. C. Cannon,[42] H. Cao,[35] L. A. Capistran,[131] E. Capocasa,[20] E. Capote,[2,11] G. Capurri,[82,81] G. Carapella,[67,132] F. Carbognani,[63] M. Carlassara,[8,9] J. B. Carlin,[124] T. K. Carlson,[133] M. F. Carney,[105] M. Carpinelli,[127,63] G. Carrillo,[78] J. J. Carter,[8,9] G. Carullo,[119,134] A. Casallas-Lagos,[135] J. Casanueva Diaz,[63] C. Casentini,[136,22] S. Y. Castro-Lucas,[137] S. Caudill,[133] M. Cavaglià,[106] R. Cavalieri,[63] A. Ceja,[54] G. Cella,[81] P. Cerdá-Durán,[138,139] E. Cesarini,[22] N. Chabbra,[34] W. Chaibi,[114] A. Chakraborty,[13] P. Chakraborty,[8,9] S. Chakraborty,[104] S. Chalathadka Subrahmanya,[98] J. C. L. Chan,[140] M. Chan,[115] K. Chang,[141] S. Chao,[142,141] P. Charlton,[143] E. Chassande-Mottin,[20] C. Chatterjee,[144] Debarati Chatterjee,[80] Deep Chatterjee,[35] M. Chaturvedi,[104] S. Chaty,[20] K. Chatziioannou,[11] A. Chen,[145] A. H.-Y. Chen,[146] D. Chen,[147] H. Chen,[142] H. Y. Chen,[148] S. Chen,[144] Yanbei Chen,[149] Yitian Chen,[121] H. P. Cheng,[150] P. Chessa,[77,51] H. T. Cheung,[91] S. Y. Cheung,[6] F. Chiadini,[151,132] G. Chiarini,[8,9,93] A. Chiba,[152] A. Chincarini,[29] M. L. Chiofalo,[82,81] A. Chiummo,[4,63] C. Chou,[146] S. Choudhary,[73] N. Christensen,[114,153] S. S. Y. Chua,[34] G. Ciani,[75,76] P. Ciecielag,[96] M. Cieślar,[125] M. Cifaldi,[22] B. Cirok,[154] F. Clara,[2] J. A. Clark,[11,57] T. A. Clarke,[6] P. Clearwater,[155] S. Clesse,[112] F. Cleva,[114,117] E. Coccia,[44,45,43] E. Codazzo,[156,157] P.-F. Cohadon,[122] S. Colace,[30] E. Colangeli,[74] M. Colleoni,[99] C. G. Collette,[158] J. Collins,[64] S. Colloms,[87] A. Colombo,[159,128] C. M. Compton,[2] G. Connolly,[78] L. Conti,[93] T. R. Corbitt,[12] I. Cordero-Carrión,[160] S. Corezzi,[77,51] N. J. Cornish,[161] I. Coronado,[162] A. Corsi,[163] R. Cottingham,[64] M. W. Coughlin,[18] A. Couineaux,[38] P. Couvares,[11,57] D. M. Coward,[73] R. Coyne,[164]

A. Cozzumbo,[44] J. D. E. Creighton,[10] T. D. Creighton,[165] P. Cremonese,[99] S. Crook,[64] R. Crouch,[2] J. Csizmazia,[2] J. R. Cudell,[166] T. J. Cullen,[11] A. Cumming,[87] E. Cuoco,[167,168] M. Cusinato,[138] L. V. Da Conceição,[169] T. Dal Canton,[41] S. Dal Pra,[170] G. Dálya,[101] B. D'Angelo,[29] S. Danilishin,[36,37] S. D'Antonio,[38] K. Danzmann,[9,8,9] K. E. Darroch,[123] L. P. Dartez,[64] R. Das,[107] A. Dasgupta,[94] V. Dattilo,[63] A. Daumas,[20] N. Davari,[171,172] I. Dave,[104] A. Davenport,[137] M. Davier,[41] T. F. Davies,[73] D. Davis,[11] L. Davis,[73] M. C. Davis,[18] P. Davis,[173,174] E. J. Daw,[175] M. Dax,[1] J. De Bolle,[95] M. Deenadayalan,[80] J. Degallaix,[176] M. De Laurentis,[32,4] F. De Lillo,[23] S. Della Torre,[128] W. Del Pozzo,[82,81] A. Demagny,[31] F. De Marco,[39,38] G. Demasi,[177,62] F. De Matteis,[21,22] N. Demos,[35] T. Dent,[178] A. Depasse,[15] N. DePergola,[103] R. De Pietri,[179,180] R. De Rosa,[32,4] C. De Rossi,[63] M. Desai,[35] R. DeSalvo,[181] A. DeSimone,[182] R. De Simone,[151,132] A. Dhani,[1] R. Diab,[46] M. C. Díaz,[165] M. Di Cesare,[32,4] G. Dideron,[183] T. Dietrich,[1] L. Di Fiore,[4] C. Di Fronzo,[73] M. Di Giovanni,[39,38] T. Di Girolamo,[32,4] D. Diksha,[37,36] J. Ding,[20,184] S. Di Pace,[39,38] I. Di Palma,[39,38] D. Di Piero,[185,48] F. Di Renzo,[56] Divyajyoti,[33] A. Dmitriev,[119] J. P. Docherty,[87] Z. Doctor,[97] N. Doerksen,[169] E. Dohmen,[2] A. Doke,[133] A. Domiciano De Souza,[186] L. D'Onofrio,[38] F. Donovan,[35] K. L. Dooley,[33] T. Dooney,[72] S. Doravari,[80] O. Dorosh,[187] W. J. D. Doyle,[123] M. Drago,[39,38] J. C. Driggers,[2] L. Dunn,[124] U. Dupletsa,[44] P.-A. Duverne,[20] D. D'Urso,[171,156] P. Dutta Roy,[46] H. Duval,[188] S. E. Dwyer,[2] C. Eassa,[2] M. Ebersold,[189,31] T. Eckhardt,[98] G. Eddolls,[79] A. Effler,[64] J. Eichholz,[34] H. Einsle,[114] M. Eisenmann,[25] M. Emma,[59] K. Endo,[152] R. Enficiaud,[1] L. Errico,[32,4] R. Espinosa,[165] M. Esposito,[4,32] R. C. Essick,[190] H. Estellés,[1] T. Etzel,[11] M. Evans,[35] T. Evstafyeva,[183] B. E. Ewing,[7] J. M. Ezquiaga,[140] F. Fabrizi,[61,62] V. Fafone,[21,22] S. Fairhurst,[33] A. M. Farah,[130] B. Farr,[78] W. M. Farr,[191,192] G. Favaro,[92] M. Favata,[193] M. Fays,[166] M. Fazio,[55] J. Feicht,[11] M. M. Fejer,[90] R. Felicetti,[185,48] E. Fenyvesi,[88,194] J. Fernandes,[195] T. Fernandes,[196,138] D. Fernando,[111] S. Ferraiuolo,[197,39,38] T. A. Ferreira,[12] F. Fidecaro,[82,81] P. Figura,[96] A. Fiori,[81,82] I. Fiori,[63] M. Fishbach,[190] R. P. Fisher,[123] R. Fittipaldi,[198,132] V. Fiumara,[199,132] R. Flaminio,[31] S. M. Fleischer,[200] L. S. Fleming,[201] E. Floden,[18] H. Fong,[115] J. A. Font,[138,139] F. Fontinele-Nunes,[18] C. Foo,[1] B. Fornal,[202] K. Franceschetti,[179] F. Frappez,[31] S. Frasca,[39,38] F. Frasconi,[81] J. P. Freed,[66] Z. Frei,[203] A. Freise,[37,108] O. Freitas,[196,138] R. Frey,[78] W. Frischhertz,[64] P. Fritschel,[35] V. V. Frolov,[64] G. G. Fronzé,[28] M. Fuentes-Garcia,[11] S. Fujii,[204] T. Fujimori,[205] P. Fulda,[46] M. Fyffe,[64] B. Gadre,[72] J. R. Gair,[1] S. Galaudage,[186] V. Galdi,[206] R. Gamba,[7] A. Gamboa,[1] S. Gamoji,[181] D. Ganapathy,[207] A. Ganguly,[80] B. Garaventa,[29] J. García-Bellido,[208] C. García-Quirós,[189] J. W. Gardner,[34] K. A. Gardner,[115] S. Garg,[42] J. Gargiulo,[63] X. Garrido,[41] A. Garron,[99] F. Garufi,[32,4] P. A. Garver,[90] C. Gasbarra,[21,22] B. Gateley,[2] F. Gautier,[209] V. Gayathri,[10] T. Gayer,[79] G. Gemme,[29] A. Gennai,[81] V. Gennari,[101] J. George,[104] R. George,[148] O. Gerberding,[98] L. Gergely,[154] Archisman Ghosh,[95] Sayantan Ghosh,[195] Shaon Ghosh,[193] Shrobana Ghosh,[8,9] Suprovo Ghosh,[210] Tathagata Ghosh,[80] J. A. Giaime,[12,64] K. D. Giardina,[64] D. R. Gibson,[201] C. Gier,[55] S. Gkaitatzis,[82,81] J. Glanzer,[11] F. Glotin,[41] J. Godfrey,[78] R. V. Godley,[8,9] O. Godwin,[11] A. S. Goettel,[33] E. Goetz,[115] J. Golomb,[11] S. Gomez Lopez,[39,38] B. Goncharov,[44] G. González,[12] P. Goodarzi,[211] S. Goode,[6] A. W. Goodwin-Jones,[15] M. Gosselin,[63] R. Gouaty,[31] D. W. Gould,[34] K. Govorkova,[35] A. Grado,[77,51] V. Graham,[87] A. E. Granados,[18] M. Granata,[176] V. Granata,[212,132] S. Gras,[35] P. Grassia,[11] J. Graves,[57] C. Gray,[2] R. Gray,[87] G. Greco,[51] A. C. Green,[37,108] L. Green,[213] S. M. Green,[74] S. R. Green,[214] C. Greenberg,[133] A. M. Gretarsson,[66] H. K. Griffin,[18] D. Griffith,[11] H. L. Griggs,[57] G. Grignani,[77,51] C. Grimaud,[31] H. Grote,[33] S. Grunewald,[1] D. Guerra,[138] D. Guetta,[215] G. M. Guidi,[61,62] A. R. Guimaraes,[12] H. K. Gulati,[94] F. Gulminelli,[173,174] H. Guo,[145] W. Guo,[73] Y. Guo,[37,36] Anuradha Gupta,[216] I. Gupta,[7] N. C. Gupta,[94] S. K. Gupta,[46] V. Gupta,[18] N. Gupte,[1] J. Gurs,[98] N. Gutierrez,[176] N. Guttman,[6] F. Guzman,[131] D. Haba,[217] M. Haberland,[1] S. Haino,[218] E. D. Hall,[35] E. Z. Hamilton,[99] G. Hammond,[87] M. Haney,[37] J. Hanks,[2] C. Hanna,[7] M. D. Hannam,[33] O. A. Hannuksela,[219] A. G. Hanselman,[130] H. Hansen,[2] J. Hanson,[64] S. Hanumasagar,[57] R. Harada,[42] A. R. Hardison,[182] S. Harikumar,[187] K. Haris,[37,72] I. Harley-Trochimczyk,[131] T. Harmark,[134] J. Harms,[44,45] G. M. Harry,[220] I. W. Harry,[74] J. Hart,[105] B. Haskell,[96,221,222] C.-J. Haster,[213] K. Haughian,[87] H. Hayakawa,[50] K. Hayama,[223] M. C. Heintze,[64] J. Heinze,[119] J. Heinzel,[35] H. Heitmann,[114] F. Hellman,[207] A. F. Helmling-Cornell,[78] G. Hemming,[63] O. Henderson-Sapir,[116] M. Hendry,[87] I. S. Heng,[87] M. H. Hennig,[87] C. Henshaw,[57] M. Heurs,[8,9] A. L. Hewitt,[224,225] J. Heynen,[15] J. Heyns,[35] S. Higginbotham,[33] S. Hild,[36,37] S. Hill,[87] Y. Himemoto,[226] N. Hirata,[25] C. Hirose,[227] D. Hofman,[176] B. E. Hogan,[66] N. A. Holland,[37,108] K. Holley-Bockelmann,[144] I. J. Hollows,[175] D. E. Holz,[130] L. Honet,[112] D. J. Horton-Bailey,[207] J. Hough,[87] S. Hourihane,[11] N. T. Howard,[144] E. J. Howell,[73] C. G. Hoy,[74] C. A. Hrishikesh,[21] P. Hsi,[35] H.-F. Hsieh,[142] H.-Y. Hsieh,[142] C. Hsiung,[228] S.-H. Hsu,[146] W.-F. Hsu,[110]

Q. Hu,[87] H. Y. Huang,[141] Y. Huang,[7] Y. T. Huang,[79] A. D. Huddart,[229] B. Hughey,[66] V. Hui,[31] S. Husa,[99] R. Huxford,[7] L. Iampieri,[39,38] G. A. Iandolo,[36] M. Ianni,[22,21] G. Iannone,[132] J. Iascau,[78] K. Ide,[230] R. Iden,[217] A. Ierardi,[44,45] S. Ikeda,[147] H. Imafuku,[42] Y. Inoue,[141] G. Iorio,[92] P. Iosif,[185,48] M. H. Iqbal,[34] J. Irwin,[87] R. Ishikawa,[230] M. Isi,[191,192] K. S. Isleif,[231] Y. Itoh,[205,232] M. Iwaya,[204] B. R. Iyer,[24] C. Jacquet,[101] P.-E. Jacquet,[122] T. Jacquot,[41] S. J. Jadhav,[233] S. P. Jadhav,[155] M. Jain,[133] T. Jain,[224] A. L. James,[11] K. Jani,[144] J. Janquart,[15] N. N. Janthalur,[233] S. Jaraba,[234] P. Jaranowski,[235] R. Jaume,[99] W. Javed,[33] A. Jennings,[2] M. Jensen,[2] W. Jia,[35] J. Jiang,[150] H.-B. Jin,[236,237] G. R. Johns,[123] N. A. Johnson,[46] M. C. Johnston,[213] R. Johnston,[87] N. Johny,[8,9] D. H. Jones,[34] D. I. Jones,[210] R. Jones,[87] H. E. Jose,[78] P. Joshi,[7] S. K. Joshi,[80] G. Joubert,[56] J. Ju,[238] L. Ju,[73] K. Jung,[239] J. Junker,[34] V. Juste,[112] H. B. Kabagoz,[64,35] T. Kajita,[240] I. Kaku,[205] V. Kalogera,[97] M. Kalomenopoulos,[213] M. Kamiizumi,[50] N. Kanda,[232,205] S. Kandhasamy,[80] G. Kang,[241] N. C. Kannachel,[6] J. B. Kanner,[11] S. A. KantiMahanty,[18] S. J. Kapadia,[80] D. P. Kapasi,[54] M. Karthikeyan,[133] M. Kasprzack,[11] H. Kato,[152] T. Kato,[204] E. Katsavounidis,[35] W. Katzman,[64] R. Kaushik,[104] K. Kawabe,[2] R. Kawamoto,[205] D. Keitel,[99] L. J. Kemperman,[116] J. Kennington,[7] F. A. Kerkow,[18] R. Kesharwani,[80] J. S. Key,[242] R. Khadela,[8,9] S. Khadka,[90] S. S. Khadkikar,[7] F. Y. Khalili,[109] F. Khan,[8,9] T. Khanam,[163] M. Khursheed,[104] N. M. Khusid,[191,192] W. Kiendrebeogo,[114,243] N. Kijbunchoo,[116] C. Kim,[244] J. C. Kim,[245] K. Kim,[246] M. H. Kim,[238] S. Kim,[247] Y.-M. Kim,[246] C. Kimball,[97] K. Kimes,[54] M. Kinnear,[33] J. S. Kissel,[2] S. Klimenko,[46] A. M. Knee,[115] E. J. Knox,[78] N. Knust,[8,9] K. Kobayashi,[204] S. M. Koehlenbeck,[90] G. Koekoek,[37,36] K. Kohri,[248,249] K. Kokeyama,[33,250] S. Koley,[44,166] P. Kolitsidou,[119] A. E. Koloniari,[251] K. Komori,[42] A. K. H. Kong,[142] A. Kontos,[252] L. M. Koponen,[119] M. Korobko,[98] X. Kou,[18] A. Koushik,[23] N. Kouvatsos,[68] M. Kovalam,[73] T. Koyama,[152] D. B. Kozak,[11] S. L. Kranzhoff,[36,37] V. Kringel,[8,9] N. V. Krishnendu,[119] S. Kroker,[253] A. Królak,[254,187] K. Kruska,[8,9] J. Kubisz,[255] G. Kuehn,[8,9] S. Kulkarni,[216] A. Kulur Ramamohan,[34] Achal Kumar,[46] Anil Kumar,[233] Praveen Kumar,[178] Prayush Kumar,[24] Rahul Kumar,[2] Rakesh Kumar,[94] J. Kume,[256,257,42] K. Kuns,[35] N. Kuntimaddi,[33] S. Kuroyanagi,[208,258] S. Kuwahara,[42] K. Kwak,[239] K. Kwan,[34] S. Kwon,[42] G. Lacaille,[87] D. Laghi,[189,101] A. H. Laity,[164] E. Lalande,[259] M. Lalleman,[23] P. C. Lalremruati,[260] M. Landry,[2] B. B. Lane,[35] R. N. Lang,[35] J. Lange,[148] R. Langgin,[213] B. Lantz,[90] I. La Rosa,[99] J. Larsen,[200] A. Lartaux-Vollard,[41] P. D. Lasky,[6] J. Lawrence,[165] M. Laxen,[64] C. Lazarte,[138] A. Lazzarini,[11] C. Lazzaro,[157,156] P. Leaci,[39,38] L. Leali,[18] Y. K. Lecoeuche,[115] H. M. Lee,[261] H. W. Lee,[262] J. Lee,[79] K. Lee,[238] R.-K. Lee,[142] R. Lee,[35] Sungho Lee,[246] Sunjae Lee,[238] Y. Lee,[141] I. N. Legred,[11] J. Lehmann,[8,9] L. Lehner,[183] M. Le Jean,[176,117] A. Lemaître,[263] M. Lenti,[62,177] M. Leonardi,[75,76,264] M. Lequime,[40] N. Leroy,[41] M. Lesovsky,[11] N. Letendre,[31] M. Lethuillier,[56] Y. Levin,[6] K. Leyde,[74] A. K. Y. Li,[11] K. L. Li,[265] T. G. F. Li,[110] X. Li,[149] Y. Li,[97] Z. Li,[87] A. Lihos,[123] E. T. Lin,[142] F. Lin,[141] L. C.-C. Lin,[265] Y.-C. Lin,[142] C. Lindsay,[201] S. D. Linker,[181] A. Liu,[219] G. C. Liu,[228] Jian Liu,[73] F. Llamas Villarreal,[165] J. Llobera-Querol,[99] R. K. L. Lo,[140] J.-P. Locquet,[110] S. C. G. Loggins,[266] M. R. Loizou,[133] L. T. London,[68] A. Longo,[61,62] D. Lopez,[166] M. Lopez Portilla,[72] M. Lorenzini,[21,22] A. Lorenzo-Medina,[178] V. Loriette,[41] M. Lormand,[64] G. Losurdo,[267,81] E. Lotti,[133] T. P. Lott IV,[57] J. D. Lough,[8,9] H. A. Loughlin,[35] C. O. Lousto,[111] N. Low,[124] N. Lu,[34] L. Lucchesi,[81] H. Lück,[9,8,9] D. Lumaca,[22] A. P. Lundgren,[268,269] A. W. Lussier,[259] R. Macas,[74] M. MacInnis,[35] D. M. Macleod,[33] I. A. O. MacMillan,[11] A. Macquet,[41] K. Maeda,[152] S. Maenaut,[110] S. S. Magare,[80] R. M. Magee,[11] E. Maggio,[1] R. Maggiore,[37,108] M. Magnozzi,[29,30] M. Mahesh,[98] M. Maini,[164] S. Majhi,[80] E. Majorana,[39,38] C. N. Makarem,[11] D. Malakar,[106] J. A. Malaquias-Reis,[19] U. Mali,[190] S. Maliakal,[11] A. Malik,[104] L. Mallick,[169,190] A.-K. Malz,[59] N. Man,[114] M. Mancarella,[100] V. Mandic,[18] V. Mangano,[171,156] B. Mannix,[78] G. L. Mansell,[79] M. Manske,[10] M. Mantovani,[63] M. Mapelli,[92,93,270] C. Marinelli,[102] F. Marion,[31] A. S. Markosyan,[90] A. Markowitz,[11] E. Maros,[11] S. Marsat,[101] F. Martelli,[61,62] I. W. Martin,[87] R. M. Martin,[193] B. B. Martinez,[131] D. A. Martinez,[54] M. Martinez,[43,271] V. Martinez,[129] A. Martini,[75,76] J. C. Martins,[19] D. V. Martynov,[119] E. J. Marx,[35] L. Massaro,[36,37] A. Masserot,[31] M. Masso-Reid,[87] S. Mastrogiovanni,[38] T. Matcovich,[51] M. Matiushechkina,[8,9] L. Maurin,[209] N. Mavalvala,[35] N. Maxwell,[2] G. McCarrol,[64] R. McCarthy,[2] D. E. McClelland,[34] S. McCormick,[64] L. McCuller,[11] S. McEachin,[123] C. McElhenny,[123] G. I. McGhee,[87] K. B. M. McGowan,[144] J. McIver,[115] A. McLeod,[73] I. McMahon,[189] T. McRae,[34] R. McTeague,[87] D. Meacher,[10] B. N. Meagher,[79] R. Mechum,[111] Q. Meijer,[72] A. Melatos,[124] C. S. Menoni,[137] F. Mera,[2] R. A. Mercer,[10] L. Mereni,[176] K. Merfeld,[163] E. L. Merilh,[64] J. R. Mérou,[99] J. D. Merritt,[78] M. Merzougui,[114] C. Messick,[10] B. Mestichelli,[44] M. Meyer-Conde,[272] F. Meylahn,[8,9] A. Mhaske,[80] A. Miani,[75,76] H. Miao,[273] C. Michel,[176] Y. Michimura,[42] H. Middleton,[119] D. P. Mihaylov,[105] A. L. Miller,[37,72] S. J. Miller,[11]

M. Millhouse,[57] E. Milotti,[185,48] V. Milotti,[92] Y. Minenkov,[22] E. M. Minihan,[66] Ll. M. Mir,[43] L. Mirasola,[156,157] M. Miravet-Tenés,[138] C.-A. Miritescu,[43] A. Mishra,[24] C. Mishra,[107] T. Mishra,[46] A. L. Mitchell,[37,108] J. G. Mitchell,[66] S. Mitra,[80] V. P. Mitrofanov,[109] K. Mitsuhashi,[25] R. Mittleman,[35] O. Miyakawa,[50] S. Miyoki,[50] A. Miyoko,[66] G. Mo,[35] L. Mobilia,[61,62] S. R. P. Mohapatra,[11] S. R. Mohite,[7] M. Molina-Ruiz,[207] M. Mondin,[181] M. Montani,[61,62] C. J. Moore,[224] D. Moraru,[2] A. More,[80] S. More,[80] C. Moreno,[135] E. A. Moreno,[35] G. Moreno,[2] A. Moreso Serra,[83] S. Morisaki,[42,204] Y. Moriwaki,[152] G. Morras,[208] A. Moscatello,[92] M. Mould,[35] B. Mours,[65] C. M. Mow-Lowry,[37,108] L. Muccillo,[177,62] F. Muciaccia,[39,38] D. Mukherjee,[119] Samanwaya Mukherjee,[24] Soma Mukherjee,[165] Subroto Mukherjee,[94] Suvodip Mukherjee,[13] N. Mukund,[35] A. Mullavey,[64] H. Mullock,[115] J. Mundi,[220] C. L. Mungioli,[73] M. Murakoshi,[230] P. G. Murray,[87] D. Nabari,[75,76] S. L. Nadji,[8,9] A. Nagar,[28,274] N. Nagarajan,[87] K. Nakagaki,[50] K. Nakamura,[25] H. Nakano,[275] M. Nakano,[11] D. Nanadoumgar-Lacroze,[43] D. Nandi,[12] V. Napolano,[63] P. Narayan,[216] I. Nardecchia,[22] T. Narikawa,[204] H. Narola,[72] L. Naticchioni,[38] R. K. Nayak,[260] L. Negri,[72] A. Nela,[87] C. Nelle,[78] A. Nelson,[131] T. J. N. Nelson,[64] M. Nery,[8,9] A. Neunzert,[2] S. Ng,[54] L. Nguyen Quynh,[276] S. A. Nichols,[12] A. B. Nielsen,[277] Y. Nishino,[25,42] A. Nishizawa,[278] S. Nissanke,[279,37] W. Niu,[7] F. Nocera,[63] J. Noller,[280] M. Norman,[33] C. North,[33] J. Novak,[117,234,281] R. Nowicki,[144] J. F. Nuño Siles,[208] L. K. Nuttall,[74] K. Obayashi,[230] J. Oberling,[2] J. O'Dell,[229] E. Oelker,[35] M. Oertel,[234,117,282,281] G. Oganesyan,[44,45] T. O'Hanlon,[64] M. Ohashi,[50] F. Ohme,[8,9] R. Oliveri,[117,282,281] R. Omer,[18] B. O'Neal,[123] M. Onishi,[152] K. Oohara,[283] B. O'Reilly,[64] M. Orselli,[51,77] R. O'Shaughnessy,[111] S. O'Shea,[87] S. Oshino,[50] C. Osthelder,[11] I. Ota,[12] D. J. Ottaway,[116] A. Ouzriat,[56] H. Overmier,[64] B. J. Owen,[284] R. Ozaki,[230] A. E. Pace,[7] R. Pagano,[12] M. A. Page,[25] A. Pai,[195] L. Paiella,[44] A. Pal,[285] S. Pal,[260] M. A. Palaia,[81,82] M. Pálfi,[203] P. P. Palma,[39,21,22] C. Palomba,[38] P. Palud,[20] H. Pan,[142] J. Pan,[73] K. C. Pan,[142] P. K. Panda,[233] Shiksha Pandey,[7] Swadha Pandey,[35] P. T. H. Pang,[37,72] F. Pannarale,[39,38] K. A. Pannone,[54] B. C. Pant,[104] F. H. Panther,[73] M. Panzeri,[61,62] F. Paoletti,[81] A. Paolone,[38,286] A. Papadopoulos,[87] E. E. Papalexakis,[211] L. Papalini,[81,82] G. Papigkiotis,[251] A. Paquis,[41] A. Parisi,[77,51] B.-J. Park,[246] J. Park,[287] W. Parker,[64] G. Pascale,[8,9] D. Pascucci,[95] A. Pasqualetti,[63] R. Passaquieti,[82,81] L. Passenger,[6] D. Passuello,[81] O. Patane,[2] A. V. Patel,[141] D. Pathak,[80] A. Patra,[33] B. Patricelli,[82,81] B. G. Patterson,[33] K. Paul,[107] S. Paul,[78] E. Payne,[11] T. Pearce,[33] M. Pedraza,[11] A. Pele,[11] F. E. Peña Arellano,[288] X. Peng,[119] Y. Peng,[57] S. Penn,[289] M. D. Penuliar,[54] A. Perego,[75,76] Z. Pereira,[133] C. Périgois,[290,93,92] G. Perna,[92] A. Perreca,[75,76,44] J. Perret,[20] S. Perriès,[56] J. W. Perry,[37,108] D. Pesios,[251] S. Peters,[166] S. Petracca,[206] C. Petrillo,[77] H. P. Pfeiffer,[1] H. Pham,[64] K. A. Pham,[18] K. S. Phukon,[119] H. Phurailatpam,[219] M. Piarulli,[101] L. Piccari,[39,38] O. J. Piccinni,[34] M. Pichot,[114] M. Piendibene,[82,81] F. Piergiovanni,[61,62] L. Pierini,[38] G. Pierra,[38] V. Pierro,[291,132] M. Pietrzak,[96] M. Pillas,[166] F. Pilo,[81] L. Pinard,[176] I. M. Pinto,[291,132,292,32] M. Pinto,[63] B. J. Piotrzkowski,[10] M. Pirello,[2] M. D. Pitkin,[224,87] A. Placidi,[51] E. Placidi,[39,38] M. L. Planas,[99] W. Plastino,[212,22] C. Plunkett,[35] R. Poggiani,[82,81] E. Polini,[35] J. Pomper,[81,82] L. Pompili,[1] J. Poon,[219] E. Porcelli,[37] E. K. Porter,[20] C. Posnansky,[7] R. Poulton,[63] J. Powell,[155] G. S. Prabhu,[80] M. Pracchia,[166] B. K. Pradhan,[80] T. Pradier,[65] A. K. Prajapati,[94] K. Prasai,[293] R. Prasanna,[233] P. Prasia,[80] G. Pratten,[119] G. Principe,[185,48] G. A. Prodi,[75,76] P. Prosperi,[81] P. Prosposito,[21,22] A. C. Providence,[66] A. Puecher,[1] J. Pullin,[12] P. Puppo,[38] M. Pürrer,[164] H. Qi,[16] J. Qin,[34] G. Quéméner,[174,117] V. Quetschke,[165] P. J. Quinonez,[66] N. Qutob,[57] R. Rading,[231] I. Rainho,[138] S. Raja,[104] C. Rajan,[104] B. Rajbhandari,[111] K. E. Ramirez,[64] F. A. Ramis Vidal,[99] M. Ramos Arevalo,[165] A. Ramos-Buades,[99,37] S. Ranjan,[57] K. Ransom,[64] P. Rapagnani,[39,38] B. Ratto,[66] A. Ravichandran,[133] A. Ray,[97] V. Raymond,[33] M. Razzano,[82,81] J. Read,[54] T. Regimbau,[31] S. Reid,[55] C. Reissel,[35] D. H. Reitze,[11] A. I. Renzini,[127,11] B. Revenu,[294,41] A. Revilla Peña,[83] R. Reyes,[181] L. Ricca,[15] F. Ricci,[39,38] M. Ricci,[38,39] A. Ricciardone,[82,81] J. Rice,[79] J. W. Richardson,[211] M. L. Richardson,[116] A. Rijal,[66] K. Riles,[91] H. K. Riley,[33] S. Rinaldi,[270] J. Rittmeyer,[98] C. Robertson,[229] F. Robinet,[41] M. Robinson,[2] A. Rocchi,[22] L. Rolland,[31] J. G. Rollins,[11] A. E. Romano,[295] R. Romano,[3,4] A. Romero,[31] I. M. Romero-Shaw,[224] J. H. Romie,[64] S. Ronchini,[7] T. J. Roocke,[116] L. Rosa,[4,32] T. J. Rosauer,[211] C. A. Rose,[57] D. Rosińska,[125] M. P. Ross,[53] M. Rossello-Sastre,[99] S. Rowan,[87] S. K. Roy,[191,192] S. Roy,[15] D. Rozza,[127,128] P. Ruggi,[63] N. Ruhama,[239] E. Ruiz Morales,[296,208] K. Ruiz-Rocha,[144] S. Sachdev,[57] T. Sadecki,[2] P. Saffarieh,[37,108] S. Safi-Harb,[169] M. R. Sah,[13] S. Saha,[142] T. Sainrat,[65] S. Sajith Menon,[215,39,38] K. Sakai,[297] Y. Sakai,[272] M. Sakellariadou,[68] S. Sakon,[7] O. S. Salafia,[159,128,127] F. Salces-Carcoba,[11] L. Salconi,[63] M. Saleem,[148] F. Salemi,[39,38] M. Sallé,[37] S. U. Salunkhe,[80] S. Salvador,[174,173] A. Salvarese,[148] A. Samajdar,[72,37] A. Sanchez,[2] E. J. Sanchez,[11] L. E. Sanchez,[11] N. Sanchis-Gual,[138] J. R. Sanders,[182] E. M. Sänger,[1] F. Santoliquido,[44,45] F. Sarandrea,[28] T. R. Saravanan,[80] N. Sarin,[6] P. Sarkar,[8,9]

A. Sasli,[251] P. Sassi,[51,77] B. Sassolas,[176] B. S. Sathyaprakash,[7,33] R. Sato,[227] S. Sato,[152] Yukino Sato,[152] Yu Sato,[152] O. Sauter,[46] R. L. Savage,[2] T. Sawada,[50] H. L. Sawant,[80] S. Sayah,[176] V. Scacco,[21,22] D. Schaetzl,[11] M. Scheel,[149] A. Schiebelbein,[190] M. G. Schiworski,[79] P. Schmidt,[119] S. Schmidt,[72] R. Schnabel,[98] M. Schneewind,[8,9] R. M. S. Schofield,[78] K. Schouteden,[110] B. W. Schulte,[8,9] B. F. Schutz,[33,8,9] E. Schwartz,[298] M. Scialpi,[299] J. Scott,[87] S. M. Scott,[34] R. M. Sedas,[64] T. C. Seetharamu,[87] M. Seglar-Arroyo,[43] Y. Sekiguchi,[300] D. Sellers,[64] N. Sembo,[205] A. S. Sengupta,[301] E. G. Seo,[87] J. W. Seo,[110] V. Sequino,[32,4] M. Serra,[38] C. K. Sethi,[320] A. Sevrin,[188] T. Shaffer,[2] U. S. Shah,[57] M. A. Shaikh,[261] L. Shao,[302] A. K. Sharma,[99] Preeti Sharma,[12] Prianka Sharma,[104] Ritwik Sharma,[18] S. Sharma Chaudhary,[106] P. Shawhan,[126] N. S. Shcheblanov,[303,263] Z.-H. Shi,[142] M. Shikauchi,[42] R. Shimomura,[304] H. Shinkai,[304] S. Shirke,[80] D. H. Shoemaker,[35] D. M. Shoemaker,[148] R. W. Short,[2] S. ShyamSundar,[104] A. Sider,[158] H. Siegel,[191,192] D. Sigg,[2] L. Silenzi,[36,37] L. Silvestri,[39,170] M. Simmonds,[116] L. P. Singer,[305] Amitesh Singh,[216] Anika Singh,[11] D. Singh,[207] N. Singh,[99] S. Singh,[217,60] A. M. Sintes,[99] V. Sipala,[171,156] V. Skliris,[33] B. J. J. Slagmolen,[34] D. A. Slater,[200] T. J. Slaven-Blair,[73] J. Smetana,[119] J. R. Smith,[54] L. Smith,[87,185,48] R. J. E. Smith,[6] W. J. Smith,[144] S. Soares de Albuquerque Filho,[61] M. Soares-Santos,[189] K. Somiya,[217] I. Song,[142] S. Soni,[35] V. Sordini,[56] F. Sorrentino,[29] H. Sotani,[306] F. Spada,[81] V. Spagnuolo,[37] A. P. Spencer,[87] P. Spinicelli,[63] A. K. Srivastava,[94] F. Stachurski,[87] C. J. Stark,[123] D. A. Steer,[307] N. Steinle,[169] J. Steinlechner,[36,37] S. Steinlechner,[36,37] N. Stergioulas,[251] P. Stevens,[41] M. StPierre,[164] M. D. Strong,[12] A. Strunk,[2] A. L. Stuver,[103,a] M. Suchenek,[96] S. Sudhagar,[96] Y. Sudo,[230] N. Sueltmann,[98] L. Suleiman,[54] K. D. Sullivan,[12] J. Sun,[241] L. Sun,[34] S. Sunil,[94] J. Suresh,[114] B. J. Sutton,[68] P. J. Sutton,[33] K. Suzuki,[217] M. Suzuki,[204] B. L. Swinkels,[37] A. Syx,[117] M. J. Szczepańczyk,[308] P. Szewczyk,[125] M. Tacca,[37] H. Tagoshi,[204] S. C. Tait,[11] K. Takada,[204] H. Takahashi,[272] R. Takahashi,[25] A. Takamori,[42] S. Takano,[309] H. Takeda,[310,311] K. Takeshita,[217] I. Takimoto Schmiegelow,[44,45] M. Takou-Ayaoh,[79] C. Talbot,[130] M. Tamaki,[204] N. Tamanini,[101] D. Tanabe,[141] K. Tanaka,[50] S. J. Tanaka,[230] S. Tanioka,[33] D. B. Tanner,[46] W. Tanner,[8,9] L. Tao,[211] R. D. Tapia,[7] E. N. Tapia San Martín,[37] C. Taranto,[21,22] A. Taruya,[312] J. D. Tasson,[153] J. G. Tau,[111] D. Tellez,[54] R. Tenorio,[99] H. Themann,[181] A. Theodoropoulos,[138] M. P. Thirugnanasambandam,[80] L. M. Thomas,[11] M. Thomas,[64] P. Thomas,[2] J. E. Thompson,[210] S. R. Thondapu,[104] K. A. Thorne,[64] E. Thrane,[6] J. Tissino,[44,45] A. Tiwari,[80] Pawan Tiwari,[44] Praveer Tiwari,[195] S. Tiwari,[189] V. Tiwari,[119] M. R. Todd,[79] M. Toffano,[92] A. M. Toivonen,[18] K. Toland,[87] A. E. Tolley,[74] T. Tomaru,[25] V. Tommasini,[11] T. Tomura,[50] H. Tong,[6] C. Tong-Yu,[141] A. Torres-Forné,[138,139] C. I. Torrie,[11] I. Tosta e Melo,[313] E. Tournefier,[31] M. Trad Nery,[114] K. Tran,[123] A. Trapananti,[52,51] R. Travaglini,[168] F. Travasso,[52,51] G. Traylor,[64] M. Trevor,[126] M. C. Tringali,[63] A. Tripathee,[91] G. Troian,[185,48] A. Trovato,[185,48] L. Trozzo,[4] R. J. Trudeau,[11] T. Tsang,[33] S. Tsuchida,[314] L. Tsukada,[213] K. Turbang,[188,23] M. Turconi,[114] C. Turski,[95] H. Ubach,[83,84] N. Uchikata,[204] T. Uchiyama,[50] R. P. Udall,[11] T. Uehara,[315] K. Ueno,[42] V. Undheim,[277] L. E. Uronen,[219] T. Ushiba,[50] M. Vacatello,[81,82] H. Vahlbruch,[8,9] N. Vaidya,[11] G. Vajente,[11] A. Vajpeyi,[6] J. Valencia,[99] M. Valentini,[108,37] S. A. Vallejo-Peña,[295] S. Vallero,[28] V. Valsan,[10] M. van Dael,[37,316] E. Van den Bossche,[188] J. F. J. van den Brand,[36,108,37] C. Van Den Broeck,[72,37] M. van der Sluys,[37,72] A. Van de Walle,[41] J. van Dongen,[37,108] K. Vandra,[103] M. VanDyke,[120] H. van Haevermaet,[23] J. V. van Heijningen,[37,108] P. Van Hove,[65] J. Vanier,[259] M. VanKeuren,[105] J. Vanosky,[2] N. van Remortel,[23] M. Vardaro,[36,37] A. F. Vargas,[124] V. Varma,[133] A. N. Vazquez,[90] A. Vecchio,[119] G. Vedovato,[93] J. Veitch,[87] P. J. Veitch,[116] S. Venikoudis,[15] R. C. Venterea,[18] P. Verdier,[56] M. Vereecken,[15] D. Verkindt,[31] B. Verma,[133] Y. Verma,[104] S. M. Vermeulen,[11] F. Vetrano,[61] A. Veutro,[38,39] A. Viceré,[61,62] S. Vidyant,[79] A. D. Viets,[89] A. Vijaykumar,[190] A. Vilkha,[111] N. Villanueva Espinosa,[138] V. Villa-Ortega,[178] E. T. Vincent,[57] J.-Y. Vinet,[114] S. Viret,[56] S. Vitale,[35] H. Vocca,[77,51] D. Voigt,[98] E. R. G. von Reis,[2] J. S. A. von Wrangel,[8,9] W. E. Vossius,[231] L. Vujeva,[140] S. P. Vyatchanin,[109] J. Wack,[11] L. E. Wade,[105] M. Wade,[105] K. J. Wagner,[111] L. Wallace,[11] E. J. Wang,[90] H. Wang,[217] J. Z. Wang,[91] W. H. Wang,[165] Y. F. Wang,[1] G. Waratkar,[195] J. Warner,[2] M. Was,[31] T. Washimi,[25] N. Y. Washington,[11] D. Watarai,[42] B. Weaver,[2] S. A. Webster,[87] N. L. Weickhardt,[98] M. Weinert,[8,9] A. J. Weinstein,[11] R. Weiss,[35] L. Wen,[73] K. Wette,[34] J. T. Whelan,[111] B. F. Whiting,[46] C. Whittle,[11] E. G. Wickens,[74] D. Wilken,[8,9,9] A. T. Wilkin,[211] B. M. Williams,[120] D. Williams,[87] M. J. Williams,[74] N. S. Williams,[1] J. L. Willis,[11] B. Willke,[9,8,9] M. Wils,[110] L. Wilson,[105] C. W. Winborn,[106] J. Winterflood,[73] C. C. Wipf,[11] G. Woan,[87] J. Woehler,[36,37] N. E. Wolfe,[35] H. T. Wong,[141] I. C. F. Wong,[219,110] K. Wong,[190] T. Wouters,[72,37] J. L. Wright,[2] M. Wright,[87,72] B. Wu,[79] C. Wu,[142] D. S. Wu,[8,9] H. Wu,[142] K. Wu,[120] Q. Wu,[53] Y. Wu,[97] Z. Wu,[101] E. Wuchner,[54] D. M. Wysocki,[10] V. A. Xu,[207] Y. Xu,[99] N. Yadav,[28] H. Yamamoto,[11]

K. Yamamoto,[152] T. S. Yamamoto,[42] T. Yamamoto,[50] R. Yamazaki,[230] T. Yan,[119] K. Z. Yang,[18] Y. Yang,[146] Z. Yarbrough,[12] J. Yebana,[99] S.-W. Yeh,[142] A. B. Yelikar,[144] X. Yin,[35] J. Yokoyama,[317,42] T. Yokozawa,[50] S. Yuan,[73] H. Yuzurihara,[50] M. Zanolin,[66] M. Zeeshan,[111] T. Zelenova,[63] J.-P. Zendri,[93] M. Zeoli,[15] M. Zerrad,[40] M. Zevin,[97] L. Zhang,[11] N. Zhang,[57] R. Zhang,[150] T. Zhang,[119] C. Zhao,[73] Yue Zhao,[162] Yuhang Zhao,[20] Z.-C. Zhao,[318] Y. Zheng,[106] H. Zhong,[18] H. Zhou,[79] H. O. Zhu,[73] Z.-H. Zhu,[318,319] A. B. Zimmerman,[148] L. Zimmermann,[56] M. E. Zucker,[35,11] and J. Zweizig[11]

(The LIGO Scientific Collaboration, the Virgo Collaboration, and the KAGRA Collaboration Collaboration)

[1]*Max Planck Institute for Gravitational Physics (Albert Einstein Institute), D-14476 Potsdam, Germany*
[2]*LIGO Hanford Observatory, Richland, Washington 99352, USA*
[3]*Dipartimento di Farmacia, Università di Salerno, I-84084 Fisciano, Salerno, Italy*
[4]*INFN, Sezione di Napoli, I-80126 Napoli, Italy*
[5]*University of Warwick, Coventry CV4 7AL, United Kingdom*
[6]*OzGrav, School of Physics & Astronomy, Monash University, Clayton 3800, Victoria, Australia*
[7]*The Pennsylvania State University, University Park, Pennsylvania 16802, USA*
[8]*Max Planck Institute for Gravitational Physics (Albert Einstein Institute), D-30167 Hannover, Germany*
[9]*Leibniz Universität Hannover, D-30167 Hannover, Germany*
[10]*University of Wisconsin-Milwaukee, Milwaukee, Wisconsin 53201, USA*
[11]*LIGO Laboratory, California Institute of Technology, Pasadena, California 91125, USA*
[12]*Louisiana State University, Baton Rouge, Louisiana 70803, USA*
[13]*Tata Institute of Fundamental Research, Mumbai 400005, India*
[14]*Centre de Physique Théorique, Aix-Marseille Université, Campus de Luminy, 163 Av. de Luminy, 13009 Marseille, France*
[15]*Université catholique de Louvain, B-1348 Louvain-la-Neuve, Belgium*
[16]*Queen Mary University of London, London E1 4NS, United Kingdom*
[17]*University of California, Davis, Davis, California 95616, USA*
[18]*University of Minnesota, Minneapolis, Minnesota 55455, USA*
[19]*Instituto Nacional de Pesquisas Espaciais, 12227-010 São José dos Campos, São Paulo, Brazil*
[20]*Université Paris Cité, CNRS, Astroparticule et Cosmologie, F-75013 Paris, France*
[21]*Università di Roma Tor Vergata, I-00133 Roma, Italy*
[22]*INFN, Sezione di Roma Tor Vergata, I-00133 Roma, Italy*
[23]*Universiteit Antwerpen, 2000 Antwerpen, Belgium*
[24]*International Centre for Theoretical Sciences, Tata Institute of Fundamental Research, Bengaluru 560089, India*
[25]*Gravitational Wave Science Project, National Astronomical Observatory of Japan, 2-21-1 Osawa, Mitaka City, Tokyo 181-8588, Japan*
[26]*Advanced Technology Center, National Astronomical Observatory of Japan, 2-21-1 Osawa, Mitaka City, Tokyo 181-8588, Japan*
[27]*Theoretisch-Physikalisches Institut, Friedrich-Schiller-Universität Jena, D-07743 Jena, Germany*
[28]*INFN Sezione di Torino, I-10125 Torino, Italy*
[29]*INFN, Sezione di Genova, I-16146 Genova, Italy*
[30]*Dipartimento di Fisica, Università degli Studi di Genova, I-16146 Genova, Italy*
[31]*Univ. Savoie Mont Blanc, CNRS, Laboratoire d'Annecy de Physique des Particules—IN2P3, F-74000 Annecy, France*
[32]*Università di Napoli "Federico II", I-80126 Napoli, Italy*
[33]*Cardiff University, Cardiff CF24 3AA, United Kingdom*
[34]*OzGrav, Australian National University, Canberra, Australian Capital Territory 0200, Australia*
[35]*LIGO Laboratory, Massachusetts Institute of Technology, Cambridge, Massachusetts 02139, USA*
[36]*Maastricht University, 6200 MD Maastricht, Netherlands*
[37]*Nikhef, 1098 XG Amsterdam, Netherlands*
[38]*INFN, Sezione di Roma, I-00185 Roma, Italy*
[39]*Università di Roma "La Sapienza", I-00185 Roma, Italy*
[40]*Aix Marseille Univ, CNRS, Centrale Med, Institut Fresnel, F-13013 Marseille, France*
[41]*Université Paris-Saclay, CNRS/IN2P3, IJCLab, 91405 Orsay, France*
[42]*University of Tokyo, Tokyo, 113-0033, Japan*
[43]*Institut de Física d'Altes Energies (IFAE), The Barcelona Institute of Science and Technology, Campus UAB, E-08193 Bellaterra (Barcelona), Spain*

[44]Gran Sasso Science Institute (GSSI), I-67100 L'Aquila, Italy
[45]INFN, Laboratori Nazionali del Gran Sasso, I-67100 Assergi, Italy
[46]University of Florida, Gainesville, Florida 32611, USA
[47]Dipartimento di Scienze Matematiche, Informatiche e Fisiche, Università di Udine, I-33100 Udine, Italy
[48]INFN, Sezione di Trieste, I-34127 Trieste, Italy
[49]Tecnologico de Monterrey, Escuela de Ingeniería y Ciencias, 64849 Monterrey, Nuevo León, Mexico
[50]Institute for Cosmic Ray Research, KAGRA Observatory, The University of Tokyo, 238 Higashi-Mozumi, Kamioka-cho, Hida City, Gifu 506-1205, Japan
[51]INFN, Sezione di Perugia, I-06123 Perugia, Italy
[52]Università di Camerino, I-62032 Camerino, Italy
[53]University of Washington, Seattle, Washington 98195, USA
[54]California State University Fullerton, Fullerton, California 92831, USA
[55]SUPA, University of Strathclyde, Glasgow G1 1XQ, United Kingdom
[56]Université Claude Bernard Lyon 1, CNRS, IP2I Lyon / IN2P3, UMR 5822, F-69622 Villeurbanne, France
[57]Georgia Institute of Technology, Atlanta, Georgia 30332, USA
[58]Chennai Mathematical Institute, Chennai 603103, India
[59]Royal Holloway, University of London, London TW20 0EX, United Kingdom
[60]Astronomical course, The Graduate University for Advanced Studies (SOKENDAI), 2-21-1 Osawa, Mitaka City, Tokyo 181-8588, Japan
[61]Università degli Studi di Urbino "Carlo Bo", I-61029 Urbino, Italy
[62]INFN, Sezione di Firenze, I-50019 Sesto Fiorentino, Firenze, Italy
[63]European Gravitational Observatory (EGO), I-56021 Cascina, Pisa, Italy
[64]LIGO Livingston Observatory, Livingston, Louisiana 70754, USA
[65]Université de Strasbourg, CNRS, IPHC UMR 7178, F-67000 Strasbourg, France
[66]Embry-Riddle Aeronautical University, Prescott, Arizona 86301, USA
[67]Dipartimento di Fisica "E.R. Caianiello", Università di Salerno, I-84084 Fisciano, Salerno, Italy
[68]King's College London, University of London, London WC2R 2LS, United Kingdom
[69]Korea Institute of Science and Technology Information, Daejeon 34141, Republic of Korea
[70]International College, Osaka University, 1-1 Machikaneyama-cho, Toyonaka City, Osaka 560-0043, Japan
[71]Accelerator Laboratory, High Energy Accelerator Research Organization (KEK), 1-1 Oho, Tsukuba City, Ibaraki 305-0801, Japan
[72]Institute for Gravitational and Subatomic Physics (GRASP), Utrecht University, 3584 CC Utrecht, Netherlands
[73]OzGrav, University of Western Australia, Crawley, Western Australia 6009, Australia
[74]University of Portsmouth, Portsmouth, PO1 3FX, United Kingdom
[75]Università di Trento, Dipartimento di Fisica, I-38123 Povo, Trento, Italy
[76]INFN, Trento Institute for Fundamental Physics and Applications, I-38123 Povo, Trento, Italy
[77]Università di Perugia, I-06123 Perugia, Italy
[78]University of Oregon, Eugene, Oregon 97403, USA
[79]Syracuse University, Syracuse, New York 13244, USA
[80]Inter-University Centre for Astronomy and Astrophysics, Pune 411007, India
[81]INFN, Sezione di Pisa, I-56127 Pisa, Italy
[82]Università di Pisa, I-56127 Pisa, Italy
[83]Institut de Ciències del Cosmos (ICCUB), Universitat de Barcelona (UB), c. Martí i Franquès, 1, 08028 Barcelona, Spain
[84]Departament de Física Quàntica i Astrofísica (FQA), Universitat de Barcelona (UB), c. Martí i Franqués, 1, 08028 Barcelona, Spain
[85]Institut d'Estudis Espacials de Catalunya, c. Gran Capità, 2-4, 08034 Barcelona, Spain
[86]Dipartimento di Medicina, Chirurgia e Odontoiatria "Scuola Medica Salernitana", Università di Salerno, I-84081 Baronissi, Salerno, Italy
[87]IGR, University of Glasgow, Glasgow G12 8QQ, United Kingdom
[88]HUN-REN Wigner Research Centre for Physics, H-1121 Budapest, Hungary
[89]Concordia University Wisconsin, Mequon, Wisconsin 53097, USA
[90]Stanford University, Stanford, California 94305, USA
[91]University of Michigan, Ann Arbor, Michigan 48109, USA
[92]Università di Padova, Dipartimento di Fisica e Astronomia, I-35131 Padova, Italy
[93]INFN, Sezione di Padova, I-35131 Padova, Italy
[94]Institute for Plasma Research, Bhat, Gandhinagar 382428, India

[95]*Universiteit Gent, B-9000 Gent, Belgium*
[96]*Nicolaus Copernicus Astronomical Center, Polish Academy of Sciences, 00-716, Warsaw, Poland*
[97]*Northwestern University, Evanston, Illinois 60208, USA*
[98]*Universität Hamburg, D-22761 Hamburg, Germany*
[99]*IAC3–IEEC, Universitat de les Illes Balears, E-07122 Palma de Mallorca, Spain*
[100]*Aix-Marseille Université, Université de Toulon, CNRS, CPT, Marseille, France*
[101]*Laboratoire des 2 Infinis—Toulouse (L2IT-IN2P3), F-31062 Toulouse Cedex 9, France*
[102]*Università di Siena, Dipartimento di Scienze Fisiche, della Terra e dell'Ambiente, I-53100 Siena, Italy*
[103]*Villanova University, Villanova, Pennsylvania 19085, USA*
[104]*RRCAT, Indore, Madhya Pradesh 452013, India*
[105]*Kenyon College, Gambier, Ohio 43022, USA*
[106]*Missouri University of Science and Technology, Rolla, Missouri 65409, USA*
[107]*Indian Institute of Technology Madras, Chennai 600036, India*
[108]*Department of Physics and Astronomy, Vrije Universiteit Amsterdam, 1081 HV Amsterdam, Netherlands*
[109]*Lomonosov Moscow State University, Moscow 119991, Russia*
[110]*Katholieke Universiteit Leuven, Oude Markt 13, 3000 Leuven, Belgium*
[111]*Rochester Institute of Technology, Rochester, New York 14623, USA*
[112]*Université libre de Bruxelles, 1050 Bruxelles, Belgium*
[113]*Bar-Ilan University, Ramat Gan, 5290002, Israel*
[114]*Université Côte d'Azur, Observatoire de la Côte d'Azur, CNRS, Artemis, F-06304 Nice, France*
[115]*University of British Columbia, Vancouver, BC V6T 1Z4, Canada*
[116]*OzGrav, University of Adelaide, Adelaide, South Australia 5005, Australia*
[117]*Centre national de la recherche scientifique, 75016 Paris, France*
[118]*Univ Rennes, CNRS, Institut FOTON—UMR 6082, F-35000 Rennes, France*
[119]*University of Birmingham, Birmingham B15 2TT, United Kingdom*
[120]*Washington State University, Pullman, Washington 99164, USA*
[121]*Cornell University, Ithaca, New York 14850, USA*
[122]*Laboratoire Kastler Brossel, Sorbonne Université, CNRS, ENS-Université PSL, Collège de France, F-75005 Paris, France*
[123]*Christopher Newport University, Newport News, Virginia 23606, USA*
[124]*OzGrav, University of Melbourne, Parkville, Victoria 3010, Australia*
[125]*Astronomical Observatory Warsaw University, 00-478 Warsaw, Poland*
[126]*University of Maryland, College Park, Maryland 20742, USA*
[127]*Università degli Studi di Milano-Bicocca, I-20126 Milano, Italy*
[128]*INFN, Sezione di Milano-Bicocca, I-20126 Milano, Italy*
[129]*Université de Lyon, Université Claude Bernard Lyon 1, CNRS, Institut Lumière Matière, F-69622 Villeurbanne, France*
[130]*University of Chicago, Chicago, Illinois 60637, USA*
[131]*University of Arizona, Tucson, Arizona 85721, USA*
[132]*INFN, Sezione di Napoli, Gruppo Collegato di Salerno, I-80126 Napoli, Italy*
[133]*University of Massachusetts Dartmouth, North Dartmouth, Massachusetts 02747, USA*
[134]*Niels Bohr Institute, Copenhagen University, 2100 København, Denmark*
[135]*Universidad de Guadalajara, 44430 Guadalajara, Jalisco, Mexico*
[136]*Istituto di Astrofisica e Planetologia Spaziali di Roma, 00133 Roma, Italy*
[137]*Colorado State University, Fort Collins, Colorado 80523, USA*
[138]*Departamento de Astronomía y Astrofísica, Universitat de València, E-46100 Burjassot, València, Spain*
[139]*Observatori Astronòmic, Universitat de València, E-46980 Paterna, València, Spain*
[140]*Niels Bohr Institute, University of Copenhagen, 2100 Kóbenhavn, Denmark*
[141]*National Central University, Taoyuan City 320317, Taiwan*
[142]*National Tsing Hua University, Hsinchu City 30013, Taiwan*
[143]*OzGrav, Charles Sturt University, Wagga Wagga, New South Wales 2678, Australia*
[144]*Vanderbilt University, Nashville, Tennessee 37235, USA*
[145]*University of Chinese Academy of Sciences / International Centre for Theoretical Physics Asia-Pacific, Bejing 100190, China*
[146]*Department of Electrophysics, National Yang Ming Chiao Tung University, 101 Univ. Street, Hsinchu, Taiwan*
[147]*Kamioka Branch, National Astronomical Observatory of Japan, 238 Higashi-Mozumi, Kamioka-cho, Hida City, Gifu 506-1205, Japan*

[148]University of Texas, Austin, Texas 78712, USA
[149]CaRT, California Institute of Technology, Pasadena, California 91125, USA
[150]Northeastern University, Boston, Massachusetts 02115, USA
[151]Dipartimento di Ingegneria Industriale (DIIN), Università di Salerno, I-84084 Fisciano, Salerno, Italy
[152]Faculty of Science, University of Toyama, 3190 Gofuku, Toyama City, Toyama 930-8555, Japan
[153]Carleton College, Northfield, Minnesota 55057, USA
[154]University of Szeged, Dóm tér 9, Szeged 6720, Hungary
[155]OzGrav, Swinburne University of Technology, Hawthorn VIC 3122, Australia
[156]INFN Cagliari, Physics Department, Università degli Studi di Cagliari, Cagliari 09042, Italy
[157]Università degli Studi di Cagliari, Via Università 40, 09124 Cagliari, Italy
[158]Université Libre de Bruxelles, Brussels 1050, Belgium
[159]INAF, Osservatorio Astronomico di Brera sede di Merate, I-23807 Merate, Lecco, Italy
[160]Departamento de Matemáticas, Universitat de València, E-46100 Burjassot, València, Spain
[161]Montana State University, Bozeman, Montana 59717, USA
[162]The University of Utah, Salt Lake City, Utah 84112, USA
[163]Johns Hopkins University, Baltimore, Maryland 21218, USA
[164]University of Rhode Island, Kingston, Rhode Island 02881, USA
[165]The University of Texas Rio Grande Valley, Brownsville, Texas 78520, USA
[166]Université de Liège, B-4000 Liège, Belgium
[167]DIFA- Alma Mater Studiorum Università di Bologna, Via Zamboni, 33–40126 Bologna, Italy
[168]Istituto Nazionale Di Fisica Nucleare—Sezione di Bologna,
viale Carlo Berti Pichat 6/2–40127 Bologna, Italy
[169]University of Manitoba, Winnipeg, MB R3T 2N2, Canada
[170]INFN-CNAF—Bologna, Viale Carlo Berti Pichat, 6/2, 40127 Bologna BO, Italy
[171]Università degli Studi di Sassari, I-07100 Sassari, Italy
[172]INFN, Laboratori Nazionali del Sud, I-95125 Catania, Italy
[173]Université de Normandie, ENSICAEN, UNICAEN, CNRS/IN2P3, LPC Caen, F-14000 Caen, France
[174]Laboratoire de Physique Corpusculaire Caen, 6 boulevard du maréchal Juin, F-14050 Caen, France
[175]The University of Sheffield, Sheffield S10 2TN, United Kingdom
[176]Université Claude Bernard Lyon 1, CNRS, Laboratoire des Matériaux Avancés (LMA),
IP2I Lyon / IN2P3, UMR 5822, F-69622 Villeurbanne, France
[177]Università di Firenze, Sesto Fiorentino I-50019, Italy
[178]IGFAE, Universidade de Santiago de Compostela, E-15782 Santiago de Compostela, Spain
[179]Dipartimento di Scienze Matematiche, Fisiche e Informatiche, Università di Parma,
I-43124 Parma, Italy
[180]INFN, Sezione di Milano Bicocca, Gruppo Collegato di Parma, I-43124 Parma, Italy
[181]California State University, Los Angeles, Los Angeles, California 90032, USA
[182]Marquette University, Milwaukee, Wisconsin 53233, USA
[183]Perimeter Institute, Waterloo, ON N2L 2Y5, Canada
[184]Corps des Mines, Mines Paris, Université PSL, 60 Bd Saint-Michel, 75272 Paris, France
[185]Dipartimento di Fisica, Università di Trieste, I-34127 Trieste, Italy
[186]Université Côte d'Azur, Observatoire de la Côte d'Azur, CNRS, Lagrange, F-06304 Nice, France
[187]National Center for Nuclear Research, 05-400 Świerk-Otwock, Poland
[188]Vrije Universiteit Brussel, 1050 Brussel, Belgium
[189]University of Zurich, Winterthurerstrasse 190, 8057 Zurich, Switzerland
[190]Canadian Institute for Theoretical Astrophysics, University of Toronto, Toronto, ON M5S 3H8, Canada
[191]Stony Brook University, Stony Brook, New York 11794, USA
[192]Center for Computational Astrophysics, Flatiron Institute, New York, New York 10010, USA
[193]Montclair State University, Montclair, New Jersey 07043, USA
[194]HUN-REN Institute for Nuclear Research, H-4026 Debrecen, Hungary
[195]Indian Institute of Technology Bombay, Powai, Mumbai 400 076, India
[196]Centro de Física das Universidades do Minho e do Porto, Universidade do Minho,
PT-4710-057 Braga, Portugal
[197]Aix Marseille Univ, CNRS/IN2P3, CPPM, Marseille, France
[198]CNR-SPIN, I-84084 Fisciano, Salerno, Italy
[199]Scuola di Ingegneria, Università della Basilicata, I-85100 Potenza, Italy
[200]Western Washington University, Bellingham, Washington 98225, USA
[201]SUPA, University of the West of Scotland, Paisley PA1 2BE, United Kingdom
[202]Barry University, Miami Shores, Florida 33168, USA
[203]Eötvös University, Budapest 1117, Hungary

[204]*Institute for Cosmic Ray Research, KAGRA Observatory, The University of Tokyo, 5-1-5 Kashiwa-no-Ha, Kashiwa City, Chiba 277-8582, Japan*
[205]*Department of Physics, Graduate School of Science, Osaka Metropolitan University, 3-3-138 Sugimoto-cho, Sumiyoshi-ku, Osaka City, Osaka 558-8585, Japan*
[206]*University of Sannio at Benevento, I-82100 Benevento, Italy and INFN, Sezione di Napoli, I-80100 Napoli, Italy*
[207]*University of California, Berkeley, California 94720, USA*
[208]*Instituto de Fisica Teorica UAM-CSIC, Universidad Autonoma de Madrid, 28049 Madrid, Spain*
[209]*Laboratoire d'Acoustique de l'Université du Mans, UMR CNRS 6613, F-72085 Le Mans, France*
[210]*University of Southampton, Southampton SO17 1BJ, United Kingdom*
[211]*University of California, Riverside, Riverside, California 92521, USA*
[212]*Dipartimento di Ingegneria Industriale, Elettronica e Meccanica, Università degli Studi Roma Tre, I-00146 Roma, Italy*
[213]*University of Nevada, Las Vegas, Las Vegas, Nevada 89154, USA*
[214]*University of Nottingham NG7 2RD, UK*
[215]*Ariel University, Ramat HaGolan St 65, Ari'el, Israel*
[216]*The University of Mississippi, University, Mississippi 38677, USA*
[217]*Graduate School of Science, Institute of Science Tokyo, 2-12-1 Ookayama, Meguro-ku, Tokyo 152-8551, Japan*
[218]*Institute of Physics, Academia Sinica, 128 Sec. 2, Academia Rd., Nankang, Taipei 11529, Taiwan*
[219]*The Chinese University of Hong Kong, Shatin, NT, Hong Kong*
[220]*American University, Washington, DC 20016, USA*
[221]*Dipartimento di Fisica, Università degli studi di Milano, Via Celoria 16, I-20133, Milano, Italy*
[222]*INFN, sezione di Milano, Via Celoria 16, I-20133, Milano, Italy*
[223]*Department of Applied Physics, Fukuoka University, 8-19-1 Nanakuma, Jonan, Fukuoka City, Fukuoka 814-0180, Japan*
[224]*University of Cambridge, Cambridge CB2 1TN, United Kingdom*
[225]*University of Lancaster, Lancaster LA1 4YW, United Kingdom*
[226]*College of Industrial Technology, Nihon University, 1-2-1 Izumi, Narashino City, Chiba 275-8575, Japan*
[227]*Faculty of Engineering, Niigata University, 8050 Ikarashi-2-no-cho, Nishi-ku, Niigata City, Niigata 950-2181, Japan*
[228]*Department of Physics, Tamkang University, No. 151, Yingzhuan Rd., Danshui Dist., New Taipei City 25137, Taiwan*
[229]*Rutherford Appleton Laboratory, Didcot OX11 0DE, United Kingdom*
[230]*Department of Physical Sciences, Aoyama Gakuin University, 5-10-1 Fuchinobe, Sagamihara City, Kanagawa 252-5258, Japan*
[231]*Helmut Schmidt University, D-22043 Hamburg, Germany*
[232]*Nambu Yoichiro Institute of Theoretical and Experimental Physics (NITEP), Osaka Metropolitan University, 3-3-138 Sugimoto-cho, Sumiyoshi-ku, Osaka City, Osaka 558-8585, Japan*
[233]*Directorate of Construction, Services & Estate Management, Mumbai 400094, India*
[234]*Observatoire Astronomique de Strasbourg, 11 Rue de l'Université, 67000 Strasbourg, France*
[235]*Faculty of Physics, University of Białystok, 15-245 Białystok, Poland*
[236]*National Astronomical Observatories, Chinese Academic of Sciences, 20A Datun Road, Chaoyang District, Beijing, China*
[237]*School of Astronomy and Space Science, University of Chinese Academy of Sciences, 20A Datun Road, Chaoyang District, Beijing, China*
[238]*Sungkyunkwan University, Seoul 03063, Republic of Korea*
[239]*Department of Physics, Ulsan National Institute of Science and Technology (UNIST), 50 UNIST-gil, Ulju-gun, Ulsan 44919, Republic of Korea*
[240]*Institute for Cosmic Ray Research, The University of Tokyo, 5-1-5 Kashiwa-no-Ha, Kashiwa City, Chiba 277-8582, Japan*
[241]*Chung-Ang University, Seoul 06974, Republic of Korea*
[242]*University of Washington Bothell, Bothell, Washington 98011, USA*
[243]*Laboratoire de Physique et de Chimie de l'Environnement, Université Joseph KI-ZERBO, 9GH2+3V5, Ouagadougou, Burkina Faso*
[244]*Ewha Womans University, Seoul 03760, Republic of Korea*
[245]*National Institute for Mathematical Sciences, Daejeon 34047, Republic of Korea*
[246]*Korea Astronomy and Space Science Institute, Daejeon 34055, Republic of Korea*

[247]Department of Astronomy and Space Science, Chungnam National University, 9 Daehak-ro, Yuseong-gu, Daejeon 34134, Republic of Korea
[248]Institute of Particle and Nuclear Studies (IPNS), High Energy Accelerator Research Organization (KEK), 1-1 Oho, Tsukuba City, Ibaraki 305-0801, Japan
[249]Division of Science, National Astronomical Observatory of Japan, 2-21-1 Osawa, Mitaka City, Tokyo 181-8588, Japan
[250]Nagoya University, Nagoya, 464-8601, Japan
[251]Department of Physics, Aristotle University of Thessaloniki, 54124 Thessaloniki, Greece
[252]Bard College, Annandale-On-Hudson, New York 12504, USA
[253]Technical University of Braunschweig, D-38106 Braunschweig, Germany
[254]Institute of Mathematics, Polish Academy of Sciences, 00656 Warsaw, Poland
[255]Astronomical Observatory, Jagiellonian University, 31-007 Cracow, Poland
[256]Department of Physics and Astronomy, University of Padova, Via Marzolo, 8-35151 Padova, Italy
[257]Sezione di Padova, Istituto Nazionale di Fisica Nucleare (INFN), Via Marzolo, 8-35131 Padova, Italy
[258]Department of Physics, Nagoya University, ES building, Furocho, Chikusa-ku, Nagoya, Aichi 464-8602, Japan
[259]Université de Montréal/Polytechnique, Montreal, Quebec H3T 1J4, Canada
[260]Indian Institute of Science Education and Research, Kolkata, Mohanpur, West Bengal 741252, India
[261]Seoul National University, Seoul 08826, Republic of Korea
[262]Department of Computer Simulation, Inje University, 197 Inje-ro, Gimhae, Gyeongsangnam-do 50834, Republic of Korea
[263]NAVIER, École des Ponts, Univ Gustave Eiffel, CNRS, Marne-la-Vallée, France
[264]Gravitational Wave Science Project, National Astronomical Observatory of Japan (NAOJ), Mitaka City, Tokyo 181-8588, Japan
[265]Department of Physics, National Cheng Kung University, No.1, University Road, Tainan City 701, Taiwan
[266]St. Thomas University, Miami Gardens, Florida 33054, USA
[267]Scuola Normale Superiore, I-56126 Pisa, Italy
[268]Institució Catalana de Recerca i Estudis Avançats, E-08010 Barcelona, Spain
[269]Institut de Física d'Altes Energies, E-08193 Barcelona, Spain
[270]Institut fuer Theoretische Astrophysik, Zentrum fuer Astronomie Heidelberg, Universitaet Heidelberg, Albert Ueberle Str. 2, 69120 Heidelberg, Germany
[271]Institucio Catalana de Recerca i Estudis Avançats (ICREA), Passeig de Lluís Companys, 23, 08010 Barcelona, Spain
[272]Research Center for Space Science, Advanced Research Laboratories, Tokyo City University, 3-3-1 Ushikubo-Nishi, Tsuzuki-Ku, Yokohama, Kanagawa 224-8551, Japan
[273]Tsinghua University, Beijing 100084, China
[274]Institut des Hautes Etudes Scientifiques, F-91440 Bures-sur-Yvette, France
[275]Faculty of Law, Ryukoku University, 67 Fukakusa Tsukamoto-cho, Fushimi-ku, Kyoto City, Kyoto 612-8577, Japan
[276]Phenikaa Institute for Advanced Study (PIAS), Phenikaa University, Yen Nghia, Ha Dong, Hanoi, Vietnam
[277]University of Stavanger, 4021 Stavanger, Norway
[278]Physics Program, Graduate School of Advanced Science and Engineering, Hiroshima University, 1-3-1 Kagamiyama, Higashihiroshima City, Hiroshima 739-8526, Japan
[279]GRAPPA, Anton Pannekoek Institute for Astronomy and Institute for High-Energy Physics, University of Amsterdam, 1098 XH Amsterdam, Netherlands
[280]University College London, London WC1E 6BT, United Kingdom
[281]Observatoire de Paris, 75014 Paris, France
[282]Laboratoire Univers et Théories, Observatoire de Paris, 92190 Meudon, France
[283]Graduate School of Science and Technology, Niigata University, 8050 Ikarashi-2-no-cho, Nishi-ku, Niigata City, Niigata 950-2181, Japan
[284]University of Maryland, Baltimore County, Baltimore, Maryland 21250, USA
[285]CSIR-Central Glass and Ceramic Research Institute, Kolkata, West Bengal 700032, India
[286]Consiglio Nazionale delle Ricerche—Istituto dei Sistemi Complessi, I-00185 Roma, Italy
[287]Department of Astronomy, Yonsei University, 50 Yonsei-Ro, Seodaemun-Gu, Seoul 03722, Republic of Korea
[288]Department of Physics, University of Guadalajara, Av. Revolucion 1500, Colonia Olimpica C.P. 44430, Guadalajara, Jalisco, Mexico
[289]Hobart and William Smith Colleges, Geneva, New York 14456, USA

[290]*INAF, Osservatorio Astronomico di Padova, I-35122 Padova, Italy*
[291]*Dipartimento di Ingegneria, Università del Sannio, I-82100 Benevento, Italy*
[292]*Museo Storico della Fisica e Centro Studi e Ricerche "Enrico Fermi", I-00184 Roma, Italy*
[293]*Kennesaw State University, Kennesaw, Georgia 30144, USA*
[294]*Subatech, CNRS/IN2P3—IMT Atlantique—Nantes Université, 4 rue Alfred Kastler BP 20722 44307 Nantes CÉDEX 03, France*
[295]*Universidad de Antioquia, Medellín, Colombia*
[296]*Departamento de Física—ETSIDI, Universidad Politécnica de Madrid, 28012 Madrid, Spain*
[297]*Department of Electronic Control Engineering, National Institute of Technology, Nagaoka College, 888 Nishikatakai, Nagaoka City, Niigata 940-8532, Japan*
[298]*Trinity College, Hartford, Connecticut 06106, USA*
[299]*Dipartimento di Fisica e Scienze della Terra, Università Degli Studi di Ferrara, Via Saragat, 1, 44121 Ferrara FE, Italy*
[300]*Faculty of Science, Toho University, 2-2-1 Miyama, Funabashi City, Chiba 274-8510, Japan*
[301]*Indian Institute of Technology, Palaj, Gandhinagar, Gujarat 382355, India*
[302]*Kavli Institute for Astronomy and Astrophysics, Peking University, Yiheyuan Road 5, Haidian District, Beijing 100871, China*
[303]*Laboratoire MSME, Cité Descartes, 5 Boulevard Descartes, Champs-sur-Marne, 77454 Marne-la-Vallée Cedex 2, France*
[304]*Faculty of Information Science and Technology, Osaka Institute of Technology, 1-79-1 Kitayama, Hirakata City, Osaka 573-0196, Japan*
[305]*NASA Goddard Space Flight Center, Greenbelt, Maryland 20771, USA*
[306]*Faculty of Science and Technology, Kochi University, 2-5-1 Akebono-cho, Kochi-shi, Kochi 780-8520, Japan*
[307]*Laboratoire de Physique de l'École Normale Supérieure, ENS, (CNRS, Université PSL, Sorbonne Université, Université Paris Cité), F-75005 Paris, France*
[308]*Faculty of Physics, University of Warsaw, Ludwika Pasteura 5, 02-093 Warszawa, Poland*
[309]*Laser Interferometry and Gravitational Wave Astronomy, Max Planck Institute for Gravitational Physics, Callinstrasse 38, 30167 Hannover, Germany*
[310]*The Hakubi Center for Advanced Research, Kyoto University, Yoshida-honmachi, Sakyou-ku, Kyoto City, Kyoto 606-8501, Japan*
[311]*Department of Physics, Kyoto University, Kita-Shirakawa Oiwake-cho, Sakyou-ku, Kyoto City, Kyoto 606-8502, Japan*
[312]*Yukawa Institute for Theoretical Physics (YITP), Kyoto University, Kita-Shirakawa Oiwake-cho, Sakyou-ku, Kyoto City, Kyoto 606-8502, Japan*
[313]*University of Catania, Department of Physics and Astronomy, Via S. Sofia, 64, 95123 Catania CT, Italy*
[314]*National Institute of Technology, Fukui College, Geshi-cho, Sabae-shi, Fukui 916-8507, Japan*
[315]*Department of Communications Engineering, National Defense Academy of Japan, 1-10-20 Hashirimizu, Yokosuka City, Kanagawa 239-8686, Japan*
[316]*Eindhoven University of Technology, 5600 MB Eindhoven, Netherlands*
[317]*Kavli Institute for the Physics and Mathematics of the Universe (Kavli IPMU), WPI, The University of Tokyo, 5-1-5 Kashiwa-no-Ha, Kashiwa City, Chiba 277-8583, Japan*
[318]*Department of Astronomy, Beijing Normal University, Xinjiekouwai Street 19, Haidian District, Beijing 100875, China*
[319]*School of Physics and Technology, Wuhan University, Bayi Road 299, Wuchang District, Wuhan, Hubei, 430072, China*
[320]*University of Cologne (Universität zu Köln), Cologne, North Rhine-Westphalia, Germany*

[a]Deceased, September 2024.